Detection of epileptic seizures from compressively sensed EEG signals for wireless body area networks

Mohammad H. Aghababaei[1], Ghasem Azemi[1*], and John M. O'Toole[2,3]

[1] Faculty of Electrical and Computer Engineering, Razi University, Kermanshah, Iran

Email: aghababaei@razi.ac.ir

[2] INFANT Research Centre, Ireland

[3] Department of Paediatrics and Child Health, University College Cork, Ireland

Email: jotoole@ucc.ie

[*]*Corresponding author*

Email: g.azemi@razi.ac.ir

Abstract

Wireless body area networks (WBANs) are gaining popularity for tele-monitoring of biomedical signals such as the electroencephalogram (EEG), with diagnosing and monitoring of epileptic seizures being one of the most important applications. Most seizure-detection algorithms cannot be applied directly to the compressed data in WBANs as they require full reconstruction of original EEG signals. In this study, we propose a novel feature for real-time automatic single-channel seizure detection which does not require complete reconstruction of original EEGs. The feature is based on iteratively applying the orthogonal matching pursuit (OMP) algorithm on the compressed EEG data and computing the rate by which the energies of partially reconstructed signals are increased. The feature, i.e. partial energy difference (PED), is then used for classifying seizure and non-seizure states. We also extend this method to the case for multichannel EEG. In multichannel case, the simultaneous OMP (SOMP) with a low number of iterations (1 and 15 iteration) is applied to the compressed data and the difference between the Frobenius norms of partially reconstructed signals is used as a multivariate feature for the classification of seizure and non-seizure states. The proposed features are used to detect seizure intervals in the EEG database provided by the University of Bonn and the CHB-MIT database. The results show that the proposed features can classify seizure epochs from non-seizures even for compression ratios as small as 0.05. The results also show that the proposed single-channel method achieves improvement of up to 4% for the area under the curve (AUC) with significantly less execution time compared to the benchmark matrix determinant (MD) classification approach. The results of applying the proposed multivariate feature to seizure and non-seizure segments of length 5 seconds from the CHB-MIT database show that it achieves mean AUC values of 0.941, 0.941, and 0.939 with mean execution times of 9.5, 10.7, and 13.1 seconds for compression ratios of 0.05, 0.1, and 0.2, respectively. Applying a threshold to the PED in a leave-one-out cross-validation (LOO-CV) scenario generates a sensitivity of 0.873,specificity of 0.710, and accuracy of 0.791 at the compression ratio of 0.05. The proposed single- and multichannel features have the potential for deployment in WBANs for the real-time tele-monitoring of epilepsy patients in healthcare applications.

Keywords: EEG; epileptic seizure; compressive sensing; wireless body area networks; partial energy difference feature

1. Introduction

A wireless body area network (WBAN) is an intelligent health monitoring system that is increasingly being used in personalized telemedicine for real-time monitoring of at-risk patients without imposing any constraints on their normal daily life activities (Antonopoulos & Voros, 2016; Movassaghi, Abolhasan, Lipman, Smith, & Jamalipour, 2014; Negra, Jemili, & Belghith, 2016; Pawar, Jones, van Beijnum, & Hermens, 2012; Silva, Rodrigues, de la Torre Díez, López-Coronado, & Saleem, 2015). Use of WBANs can drastically reduce health care costs by removing costly in-hospital monitoring of patients. These systems are composed of small, wearable, battery-powered sensors that are implanted, embedded inside, or placed on the body of the patients. The sensors are wired to a central microprocessor where the data are compressed and sent to a local smartphone. The smartphone transmits the compressed data over the internet to a remote medical terminal (e.g., a hospital) where the data are monitored and analyzed to determine the appropriate course of action. WBANs can be deployed for tele-monitoring of various types of biomedical signals such as the electroencephalogram (EEG) and electrocardiogram (ECG).

EEG is a non-invasive electrophysiological technique for monitoring the electrical activity of the brain and the most common test for diagnosing epilepsy. Epilepsy is a neurological disorder that affects around 50 million people worldwide. If diagnosed and treated properly, up to 70% of people with epilepsy could live seizure-free ("World Health Organization," 2001). Identifying seizure events in long-duration EEG recordings is a time-consuming and a burdensome task for medical experts. Automated systems to detect seizures would enable rapid identification without the need for visually scoring long EEG records. In addition, an automated system would enable real-time detection of seizures, something not practical with the visual review of the EEG.

There are 2 main constraints in designing a WBAN-based EEG monitoring system for seizure detection. The 1st constraint is the limit on energy consumed in EEG sensing and energy consumed in the compression and transmission of the acquired signals. Energy can be conserved by applying compressed sensing (CS) techniques that efficiently compress the EEG and reduce processing during sampling and also conserve energy during transmission by using appropriate sensing matrices and compression ratios.

The 2nd constraint on an EEG seizure detection WBAN system is the processing time and also the quality of the reconstructed multichannel signals. However, existing automatic seizure detection methods cannot be directly applied to the compressed data in WBANs and, prior to applying such detection algorithms, the original EEGs need to be fully reconstructed from compressive measurements. The reconstruction stage in CS is a time-consuming procedure with high computational complexity. Therefore, for real-time applications of WBANs for tele-monitoring of EEGs, there is a need for developing fast and efficient automatic seizure detection methods which do not require full reconstruction of the original signals. This study is an initial step towards this goal.

Generally, 3 approaches can be used in wireless EEG-based seizure detection systems. The 1st approach is the transmission of the entire raw EEG data and use of one of the many accurate algorithms in the literature for detecting

seizures. There are many recent works in the literature that have studied the epileptic seizure detection, including: deep learning methods (Hossain, Amin, Alsulaiman, & Muhammad, 2019; Kaleem, Gurve, Guergachi, & Krishnan, 2018; Sharma, Sircar, & Pachori, 2019; Zabihi M Fau - Kiranyaz, Kiranyaz S Fau - Jantti, Jantti V Fau - Lipping, Lipping T Fau - Gabbouj, & Gabbouj, 2020), filter bank methods (Bhati, Pachori, Sharma, & Gadre, 2020; Dinesh, Akruti, Ram Bilas, & Vikram, 2020; Nishad & Pachori, 2020; Serna, Paternina, Zamora-Méndez, Tripathy, & Pachori, 2020), empirical mode decomposition methods (K.C. Santosh), and entropy methods (V. Gupta & Pachori, 2019; Sharma et al., 2019). A recently proposed method that uses the matrix determinant (MD) of EEG signals as a feature, outperforms most state-of-the-art methods in terms of the seizure detection performance as well as the execution time (Raghu, Sriraam, Hegde, & Kubben, 2019). This method, explained in Section 2, is used as the benchmark when evaluating the performance of the proposed single-channel feature in this study. However, transmitting raw EEG data requires high-energy consumption at the sensor node and large bandwidth and therefore this 1st approach is not suitable for WBANs.

Another approach is to extract suitable features from raw EEG data at the sensor node and transmit those EEG features to the remote terminal for the classification purpose. Recent methods which use this approach are presented in (Chiang & Ward, 2014; Hussein, Mohamed, & Alghoniemy, 2015). Despite energy conservation in both data encoding and transmission, these approaches have shown low efficacy in seizure detection. Furthermore, because the feature extraction in this scheme is done at the sensor node, very simple features (with low computational loads) should be selected since complex features consume large power from the sensors which leads to a reduction in the lifetime of the batteries.

Finally, the 3rd approach is to transmit the compressed EEG data. However, in the context of WBAN systems, the traditional methods for compressing the EEG signals such as set partitioning in hierarchical trees (Said & Pearlman, 1996) cannot be used due to their high complexity and computational loads. As an alternative method, for reducing the processing load as well as the transmission energy in WBANs, CS can be used for efficient compression of EEG signals (Chiang & Ward, 2014; Zeng et al., 2016). Power consumption in WBANs can be significantly reduced by using such CS techniques, while maintaining high seizure detection performance. In (Zeng et al., 2016), the altered EEG compressibility (i.e., the reconstruction performance in terms of normalized mean squared error (NMSE) and structural similarity (SSIM)) is used as a feature to classify EEG signals in seizure-free, pre-seizure, and seizure states. The results of this study show that both CS-NMSE and CS-SSIM outperform the sample entropy and permutation entropy in epileptic seizure classification and are therefore good biomarkers for diagnosing seizure states. To the best of the authors' knowledge, all of the studies in the literature related to the seizure detection in CS-based WBAN systems based on this 3rd approach, need recovery of the full (original) EEG samples at the remote terminal (Chiang & Ward, 2014; Zeng et al., 2016). However, the high computational cost involved in the recovery of high-quality signals limits the utility of such methods for real-time seizure detection. The primary objective of this study was to develop a seizure detection method for a WBAN system using CS to operate with low complexity and therefore without the need to fully reconstruct the EEG signal. We do so by defining a feature with low complexity from a

limited number of iterations of the reconstruction process. Methods are proposed for both single-channel and multichannel EEG.

2. Materials and methods

In this section, we first describe the 2 EEG databases, i.e. the Bonn University and the CHB-MIT databases, used in this study for evaluating the performance of the proposed univariate and multivariate seizure detection features. Next, we review the fundamentals of CS of EEG signals and conventional seizure classification methods in CS-based WBAN systems. Finally, we present the univariate and multivariate features, which we refer to as the partial energy difference (PED), for real-time automatic seizure detection.

2.1. EEG databases

In this study, 2 publicly available EEG databases are used. The 1st one is the database provided by the University of Bonn. This database consists of 5 different datasets of single-channel EEG recordings, namely, A, B, C, D, and E (also referred to as Z, O, N, F, and S). Each dataset composed of 100 EEG segments sampled at 173.61 Hz and 23.6 seconds long, i.e. 4097 samples, acquired from 5 subjects aged 19-60. Sample EEG signals of length 23.6 seconds from these datasets are shown in Figure 1. The bandwidth of the data recording system is from 0.5 to 85 Hz. The first 2 datasets (i.e. datasets A and B) were recorded from the scalp of healthy subjects according to the 10-20 international standard electrode positioning system with eyes open (Dataset A) and eyes closed (Dataset B). Datasets C, D and E are intracranial EEGs of epilepsy patients. EEGs in both datasets C and D were acquired during interictal (seizure-free) intervals while Dataset E contains EEGs acquired from epileptic volunteers during ictal period (seizure). We acknowledge the limitation of comparing seizure and non-seizure among different participants, however this is one of the few databases freely available with per-channel annotations. In addition, this database has been (and is still being) used to develop and test many other seizure detection methods (Bhati et al., 2020; Dinesh et al., 2020; A. Gupta, Singh, & Karlekar, 2018; V. Gupta, Bhattacharyya, & Pachori, 2020; V. Gupta & Pachori, 2019; Nishad & Pachori, 2020; Rahul, Pradip, & Ram Bilas, 2020; Richhariya & Tanveer, 2018; Serna et al., 2020; Sharma et al., 2019) and therefore is a useful benchmark database. Table 1 describes the database; more details about this database can be found in (R. Andrzejac, 2001).

Table 1. Specifications of the 5 EEG datasets in the Bonn University EEG database. All the datasets consist of 100 segments of length 23.6 seconds.

Datasets	Dataset A	Dataset B	Dataset C	Dataset D	Dataset E
Subjects	5 healthy	5 healthy	5 epileptic patients	5 epileptic patients	5 epileptic patients
Subject's state	Awake state with eyes open (normal)	Awake state with eyes closed (normal)	Interictal (seizure-free)	Interictal (seizure-free)	Ictal (seizure activity)
Electrode type	Surface	Surface	Intracranial	Intracranial	Intracranial
Electrode placement	International 10-20 system	International 10-20 system	Hippocampal formation	Epileptogenic zone	Epileptogenic zone

In this study, 4 different binary classification experiments for differentiating between non-epileptic and epileptic states, as explained below, are considered. The selection of these experiments is based on their clinical significance and to allow for comparison with published work. The experiments are as follows:

1. {A}-{E}: classification of recordings from epileptic patients during seizure intervals (E) and recordings from healthy subjects with eyes open condition (A).

2. {B}-{E}: classification of recordings between healthy subjects with eyes closed condition (B) and recordings from epileptic patients during seizure intervals (E).

3. {C}-{E}: classification of recordings from epileptic patients during seizure-free intervals (recorded from the hippocampal formation-(C)) and seizure intervals (E).

4. {D}-{E}: classification of recordings from epileptic patients during seizure-free intervals (recorded from the epileptogenic zone-(D)) and seizure intervals (E) .

The 2nd database consists of multichannel EEG recordings acquired from 22 subjects (5 males, aged 3-22 and 17 females aged 1.5-19) at the Children Hospital Boston, Massachusetts Institute of Technology (CHB-MIT). These recordings are grouped into 23 cases, chb01-chb23; case chb21 was obtained 1.5 years after chb01 from Subject 01. For each subject, there are between 9 and 42 separate recordings. Electrodes are placed according to the international 10-20 system of electrode placement and EEG sampled at 256Hz. In most recordings there are 23 common bipolar EEG channels. These channels are: FP1-F7, F7-T7, T7-P7, P7-O1, FP1-F3, F3-C3, C3-P3, P3-O1, FP2-F4, F4-C4, C4-P4, P4-O2, FP2-F8, F8-T8, T8-P8, P8-O2, FZ-CZ, CZ-PZ, P7-T7, T7-FT9, FT9-FT10, FT10-T8, and T8-P8. For most subjects, recordings have exactly 1 hour duration, however, in some cases they are up to 4 hours long. Table 2 describes this database. For evaluating the performance of the proposed multivariate feature for seizure detection, we selected the datasets with the same bipolar montage which contained at least 5 minutes of seizure activity, resulting in 11 multichannel EEG datasets acquired from 11 subjects. EEGs of Subject 13 was excluded due to the presence of bursts in the recordings (Shoeb, September 2009). More details about this database can be found in (Shoeb, September 2009). Figure 2 shows an example of seizure and non-seizure EEG.

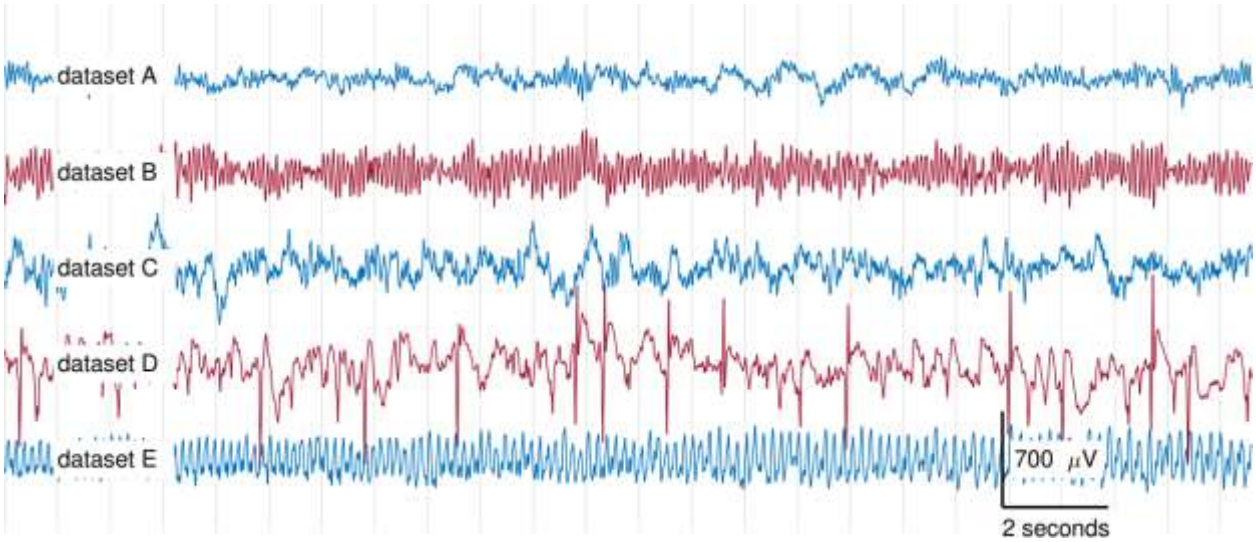

Figure 1. Sample EEG signals of length 23.6 seconds selected from 5 different datasets A, B. C, D, and E of the Bonn University database. Datasets A and B are scalp EEG recordings and datasets C to E are intracranial EEGs.

Table 2. Details of the EEG datasets in the CHB-MIT database. Selected subjects are shown in red and also marked with asterisk. (Criteria for selection was > 5 minutes of seizure activity and a common 23 channel montage.)

Subject ID	Gender	Age	Number of seizures	Total seizure duration (seconds)
*Subject 01	F	11	7	442
Subject 02	M	11	3	172
*Subject 03	F	14	7	402
*Subject 04	M	22	4	378
*Subject 05	F	7	5	558
Subject 06	F	1.5	10	153
*Subject 07	F	14.5	3	325
*Subject 08	M	3.5	5	919
Subject 09	F	10	4	276
*Subject 10	M	3	7	447
*Subject 11	F	12	3	806
Subject 12	F	2	27	988
Subject 13	F	3	12	535
Subject 14	F	9	8	168
Subject 15	M	16	20	1992
Subject 16	F	7	8	68
Subject 17	F	12	3	292
*Subject 18	F	18	6	317
Subject 19	F	19	3	236
Subject 20	F	6	8	292
Subject 21	F	13	4	196
Subject 22	F	9	3	204
*Subject 23	F	6	7	424

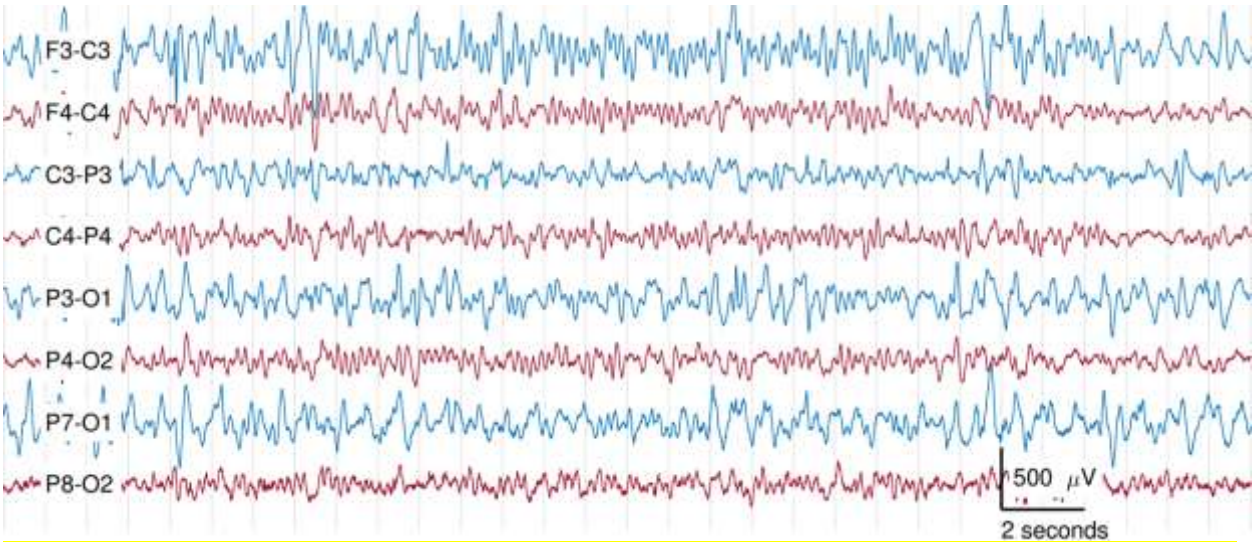

(a)

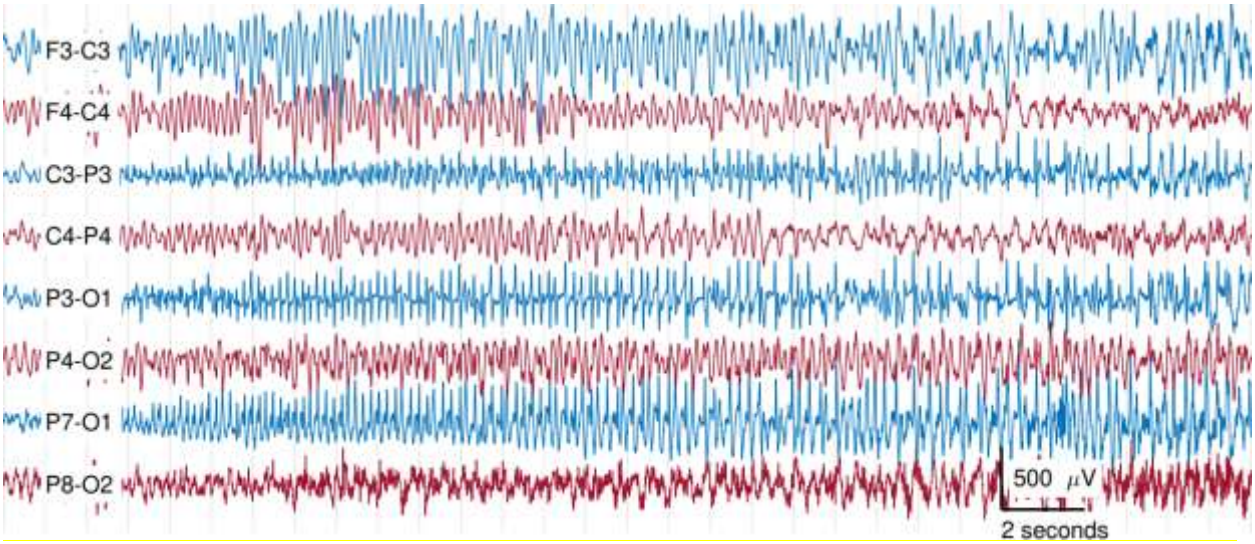

(b)

Figure 2. Sample multichannel EEG signals: a 30 seconds segment of (a) non-seizure and (b) seizure from the recordings of Subject 05 of the CHB-MIT database. To enhance clarity, only 8 of the 23 channels in the original montage are plotted.

2.2. Compressed sensing of EEG signals

2.2.1. Fundamentals of CS of single-channel EEG signals

Compressed sensing (CS) is a near-lossless data compression technique that has received a lot of attention over the past decade. By exploiting the signal's sparsity in an appropriate sparsity domain, we can recover the original signal from its compressive measurements with high probability (with small error).

Let $\boldsymbol{x} \in \mathbb{R}^{N\times 1}$ denotes the original single-channel EEG signal with N being the epoch length (number of samples of the signal). Suppose the vector $\boldsymbol{y} \in \mathbb{R}^{M\times 1}$ contains linear measurements of the signal $\boldsymbol{x}$, where M is the number of measurements with $M \ll N$. The relationship between $\boldsymbol{x}$ and $\boldsymbol{y}$ in the CS framework is given by:

$$\boldsymbol{y} = \boldsymbol{\Phi x}, \tag{1}$$

where $\boldsymbol{\Phi} \in \mathbb{R}^{M \times N}$ is the measurement/projection/sensing matrix. The compression ratio (CR) of the CS technique is defined as:

$$CR = {}^{M}/_{N}. \tag{2}$$

One can recover the original signal $\boldsymbol{x}$ from its compressive measurements $\boldsymbol{y}$ according to (Candes & Wakin, 2008):

$$\hat{\boldsymbol{x}} = \arg\min_{\boldsymbol{x}} \|\boldsymbol{y} - \boldsymbol{\Phi x}\|_2^2 + \lambda \|\boldsymbol{x}\|_1, \tag{3}$$

in which λ is a regularization parameter and $\|.\|_p$ ($p \geq 1$ is a real number) for the vector $\boldsymbol{a} = \{a_i\}_{i=1}^{n}$ is defined as:

$$\|\boldsymbol{a}\|_p = \left(\sum_{i=1}^{n} |a_i|^p \right)^{\frac{1}{p}}. \tag{4}$$

Due to the underdetermined nature of (1), the reconstruction of the original EEG signal $\boldsymbol{x}$ from its compressive measurements $\boldsymbol{y}$ is an ill-conditioned problem. But, it has been shown that if $\boldsymbol{x}$ is sufficiently sparse or compressible[1] in an appropriate transform domain, one can recover it with small error under certain condition on the sensing matrix $\boldsymbol{\Phi}$ (Candes, Romberg, & Tao, 2006; Candes & Tao, 2006; Donoho, 2006). The signal $\boldsymbol{x}$ is said to be a sparse or compressible in the transform domain $\boldsymbol{\Psi} \in \mathbb{R}^{N \times N}$ (known as sparsifying/dictionary matrix) if we have:

$$\boldsymbol{\alpha} = \boldsymbol{\Psi x}, \tag{5}$$

where $\boldsymbol{\alpha} \in \mathbb{R}^{N \times 1}$ is a sparse or compressible signal.

2.2.2. Fundamentals of CS of multichannel EEG signals

Consider the original EEG matrix $\boldsymbol{X} \in \mathbb{R}^{N \times CH}$ where N is the epoch length and CH is the number of EEG channels. In this case, the multichannel counterpart of (1) is given by (Aghababaei & Azemi, 2020):

$$\boldsymbol{Y} = \boldsymbol{\Phi X}, \tag{6}$$

where $\boldsymbol{Y} \in \mathbb{R}^{M \times CH}$ contains the compressive measurements.

The original EEG matrix $\boldsymbol{X}$ can be reconstructed from the compressive measurements $\boldsymbol{Y}$ according to (Kamal, Shoaran, Leblebici, Schmid, & Vandergheynst, 2013):

$$\hat{\boldsymbol{X}} = \min_{\boldsymbol{X}} \|\boldsymbol{Y} - \boldsymbol{\Phi \Psi}^T \boldsymbol{X}\|_F^2 + \lambda \|vec(\boldsymbol{X})\|_1, \tag{7}$$

[1] Note that a sparse signal is a signal that most of its elements are zero and a compressible signal is defined as a signal that most of its elements have small values (i.e. close to zero).

where $vec(\boldsymbol{X})$ is a vector that is formed by column-wise stacking of the elements of the matrix $\boldsymbol{X}$, and $\|\boldsymbol{A}\|_F$ is the Frobenius norm which it defines for the matrix $\boldsymbol{A} \in \mathbb{R}^{m\times n}$ as follows:

$$\|\boldsymbol{A}\|_F = \sqrt{\sum_{i=1}^{m}\sum_{j=1}^{n}|a_{ij}|^2}. \tag{8}$$

Since nearby EEG channels record the neural activities produced by the same source(s) and also due to the volume conduction effect, there are high value of correlation between these channels, especially for referential montages. Thus, these signals have similar signatures in the transform (sparsifying) domain, i.e. high values of these signals in the transform domain occur in same positions, and therefore matrix $\boldsymbol{X}$ will be a row-sparse matrix in the transform domain (Aghababaei & Azemi, 2020). Thus one can achieve high recovery accuracy by exploiting these correlations in the reconstruction procedure (Aghababaei & Azemi, 2020).

2.2.3. Choosing the sensing and sparsifying matrices

It is well known that for achieving a high recovery accuracy in the CS, $\boldsymbol{\Phi}$ and $\boldsymbol{\Psi}$ should have a low mutual coherence value defined as (Candes & Wakin, 2008):

$$\mu(\boldsymbol{\Phi},\boldsymbol{\Psi}) = \sqrt{N}\max_{1\le k,j\le N}\left|\langle \boldsymbol{\varphi_k},\boldsymbol{\psi_j}\rangle\right|, \tag{9}$$

where $\boldsymbol{\varphi_k}$ and $\boldsymbol{\psi_j}$ are the k^{th} and j^{th} columns of the matrices $\boldsymbol{\Phi}$ and $\boldsymbol{\Psi}$, respectively. It is also known that random matrices with independent identically distributed (i.i.d.) entries have low coherence value with any deterministic matrices (Candes & Wakin, 2008).

There are 2 very popular random sensing matrices that are used in the CS of biomedical signals: random Gaussian and random binary matrices. The random Gaussian sensing matrices have been used as measurement matrices in the CS of EEG signals (Abdulghani, Casson, & Rodriguez-Villegas, 2012; Aviyente, 2007). However, generation of such matrices in WBAN systems is computationally expensive and not energy efficient; hence, the use of these matrices in WBANs are not recommended. The random binary sensing matrices, introduced in (Gilbert & Indyk, 2010), can overcome these shortcomings. In these matrices, each column has only 'd' 1s at random locations and other entries are 0 and, therefore, only few additions and no multiplication are performed to produce measurements. Choosing small value for d can significantly reduce the computational loads of the WBAN system and leads to small size batteries for sensor nodes. In (Aghababaei & Azemi, 2020; Mohsina & Majumdar, 2013), random binary matrices are used as measurement matrices for the CS of EEG signals in WBAN systems. This paper also uses the random binary matrix as the sensing matrix.

As for the sparsity domain, it is known that EEG signals are not sparse or compressible in the original time domain. But, there are 3 popular sparsity domains for them: wavelet (Kamal et al., 2013; Majumdar, Shukla, & Ward, 2015), Gabor (Aviyente, 2007; Mohsina & Majumdar, 2013), and discrete cosine transform (DCT) (Aghababaei & Azemi,

2020; Zhang, Jung, Makeig, & Rao, 2013) domains. Following the results presented in (Aghababaei & Azemi, 2020; Zhang et al., 2013), this study chooses the DCT as the sparsity domain for EEG signals.

2.2.4. Recovery algorithms

There are 4 classes of recovery algorithms that are used in the CS field. The 1st class includes the convex relaxation algorithms that solve a convex optimization problem based on linear programming. Basis pursuit de-noising (BPDN) (Chen, Donoho, & Saunders, 1998) and least absolute shrinkage and selection operator (LASSO) (Tibshirani, 1996) are 2 most popular algorithms in this class.

The 2nd class of recovery methods comprises of greedy iterative algorithms. Orthogonal matching pursuit (OMP) (J. A. Tropp & Gilbert, 2007) and compressive sampling matching pursuit (CoSaMP) (Needell & Tropp, 2009) are 2 most common examples in this class that they are designed for solving the single measurement vector recovery problems. The multivariate counterpart of the OMP algorithm that solves the multiple measurement vector recovery problems is the simultaneous OMP (SOMP) algorithm (Joel A. Tropp, Gilbert, & Strauss, 2006). The main property of greedy algorithms is that they are very fast and have low computational costs. In this study, the well-known OMP and SOMP algorithms are used with the aim of achieving the real-time signal processing goal.

The 3rd class consists of iterative thresholding algorithms which use soft or hard thresholding to recover the original signals. Message passing and expander matching pursuits are 2 popular algorithms in this class (Qaisar, Bilal, Iqbal, Naureen, & Lee, 2013).

The 4th class of recovery algorithms assume a block structure for the original signals. Block orthogonal matching pursuit (Block-OMP) (Eldar, Kuppinger, & Bolcskei, 2010) and block sparse Bayesian learning (BSBL) (Zhang & Rao, 2013) are 2 most common examples. The BSBL algorithm which also exploits the intra-block correlation, has shown high recovery performance even for signals with no block structure such as EEG signals (Zhang et al., 2013). In (Chiang & Ward, 2014; Zeng et al., 2016), this algorithm is used for accurate reconstruction of the original EEG signals from compressive measurements for diagnosing seizure states. Therefore, in this paper, following (Chiang & Ward, 2014; Zeng et al., 2016), this algorithm is used to reconstruct the original EEG samples from their compressive measurements before applying the MD (matrix determinant) classification approach (the best performing single-channel seizure detection method described in Section 2.3.2). The results of applying the MD classification method to fully reconstructed EEG signals (from compressive measurements) using the BSBL recovery algorithm is used in Section 3 as a benchmark for evaluating the performance of the proposed single-channel method in this paper.

2.3. Automatic seizure detection in CS-based WBAN systems

2.3.1. Traditional wireless seizure detection approach

The traditional epileptic seizure detection approach for WBANs, as shown in Figure 3 (Top), is comprised of 2 subsystems: a wireless sensor node and a data server node. After acquiring the raw EEG data at the sensor node, the

compressive measurements are obtained by applying (1) to the data. The compressed data are then wirelessly transmitted to the server node. At the server node, first the full original EEG samples are reconstructed from the received compressive measurements and then the features relevant to seizures are extracted from the fully reconstructed EEG signals. Numerous features have been presented in the literature for automatic seizure detection applications. A thorough review of such features can be found in (Raghu et al., 2019) where a new feature based on the EEG matrix determinant (MD) is also presented. Finally, a classifier is used to classify different states based on the extracted features. Due to the high computational costs of recovery procedure in the CS, this seizure detection approach is not suitable for real-time applications.

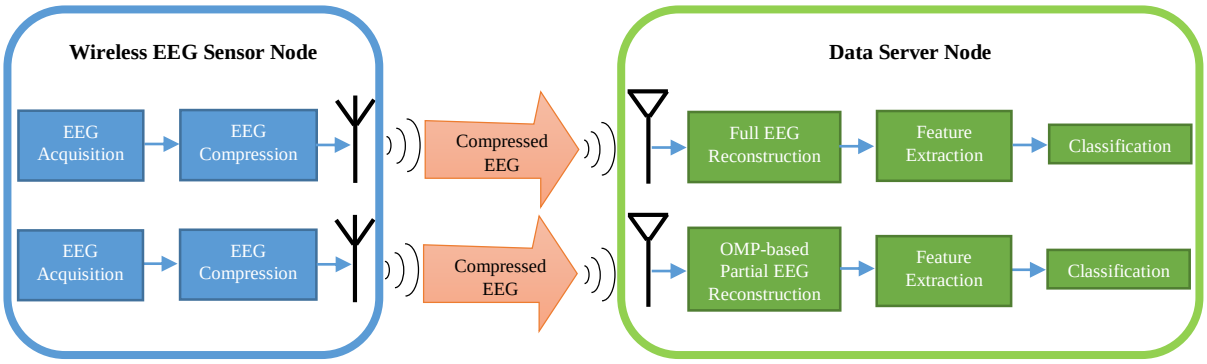

Figure 3. Automatic seizure classification in CS-based WBAN systems. (**Top**) conventional seizure detection methods. (**Bottom**) our proposed approach.

2.3.2. Matrix determinant (MD) classification method

In (Raghu et al., 2019), an automatic single-channel seizure detection method is developed and shown to outperform the most state-of-the-art methods in terms of both detection accuracy as well as the execution time. The method uses the EEG matrix determinant as a feature to capture the variations of the EEG signal amplitude with respect to time. In this method, the artifact-free filtered EEG time series are arranged sequentially to form a squared matrix and then the determinant of this matrix is calculated. The total number of elements in the squared matrix represents the epoch length.

Let us consider an EEG epoch of length T where T is a perfect square number:

$$\boldsymbol{x} = \{x_1, x_2, \dots, x_T\}. \tag{10}$$

First, each element of the vector $\boldsymbol{x}$ is replaced with its absolute square and then the resulted signal vector is arranged sequentially in a $t \times t$ squared matrix $\boldsymbol{A}$ as:

$$\boldsymbol{A} = \begin{bmatrix} x_1 & \cdots & x_t \\ \vdots & \ddots & \vdots \\ x_{((t-1)\times t)+1} & \cdots & x_T \end{bmatrix}, \tag{11}$$

where $t = \sqrt[2]{T}$.

Finally, the base 10 logarithm of the absolute value of the determinant of matrix $\boldsymbol{A}$ is calculated as:

$$Determinant = \log_{10}|\boldsymbol{A}|. \quad (12)$$

The MD method uses this value as a feature to differentiate the seizure from non-seizure intervals. More details about this approach can be found in (Raghu et al., 2019).

2.4. Partial energy difference (PED): a feature for detecting seizures in compressed EEGs

2.4.1. Univariate version of the proposed feature

As mentioned earlier, the traditional seizure detection approaches in CS-based WBAN systems need the reconstruction of full EEG samples which is computationally expensive and therefore not suitable for real-time seizure detection in WBANs. However, as shown in Figure 3 (Bottom), the proposed method can overcome this limitation by partially reconstructing EEG samples using the OMP algorithm.

The OMP algorithm is the most popular greedy algorithm in the field of sparse recovery. The original form of this algorithm is given below; more details can be found in (J. A. Tropp & Gilbert, 2007).

Algorithm 1. The orthogonal matching pursuit algorithm.

Inputs:

- An M × 1 measurement vector $\mathbf{y}$
- An M × N sensing matrix $\boldsymbol{\Phi}$
- An N × N sparsifying matrix $\boldsymbol{\Psi}$
- The sparsity level K of the original signal

Output:

- The estimated N × 1 signal $\hat{\mathbf{x}}$

Procedure:

1. Initialize the residual $\mathbf{r_0} = \mathbf{y}$, the estimated signal $\hat{\mathbf{x}}_\mathbf{0} = \mathbf{0}$, the index set $\Omega_0 = \emptyset$, the iteration counter $t = 1$, and the N × 1 transform domain coefficient vector $\widehat{\mathbf{X}} = \mathbf{0}$.
2. Calculate the new matrix $\mathbf{A} = \boldsymbol{\Phi}\boldsymbol{\Psi}'$ where $\boldsymbol{\Psi}'$ is the transpose of the matrix $\boldsymbol{\Psi}$.
3. Find the index λ_t that solves the optimization problem: $\lambda_t = \arg\max_{j=1,2,\ldots,N} |\mathbf{r_{t-1}}\mathbf{A}'_j|$ where $\boldsymbol{A}_j$ is the j[th] column of the matrix $\boldsymbol{A}$.
4. Update the index set: $\Omega_t = \Omega_{t-1} \cup \{\lambda_t\}$.
5. Update the coefficients: $\mathbf{a_t} = \mathbf{A}^{\dagger}_{\Omega_t}\mathbf{y}$ where $\mathbf{B}^{\dagger}$ represents the pseudo inverse of the matrix $\mathbf{B}$ and $\boldsymbol{B}_\Omega$ represents the columns of $\boldsymbol{B}$ that Ω shows.
6. Update the residual: $\mathbf{r_t} = \mathbf{y} - \mathbf{A}_{\Omega_t}\mathbf{a_t}$.
7. Increment the iteration counter by 1: $t = t + 1$.
8. If t is less than $K + 1$, go to Step 3.
9. Update the transform domain coefficient vector: $\widehat{\mathbf{X}}_\mathbf{\Omega} = \mathbf{a_t}$.
10. Calculate the estimated signal: $\hat{\mathbf{x}} = \boldsymbol{\Psi}'\widehat{\mathbf{X}}$.

By running the OMP algorithm P times with the sparsity levels[2] $K = 1,2,3,\ldots,P$ and then calculating the energy of the estimated signals at each run, i.e. the partial energy, it can be seen that the distribution of the partial energy for the seizure and non-seizure segments are very different. (Sparsity level is equal to the number of iterations of the OMP.)

[v] It should be noted that the number of iterations in the OMP algorithm is the same as the sparsity level.

For illustration, Figure 4 shows the distribution of partial energies as a function of the sparsity level for 2 EEG segments chosen from the Dataset A (normal) and Dataset E (seizure) of the Bonn University database introduced in Section 2.1.

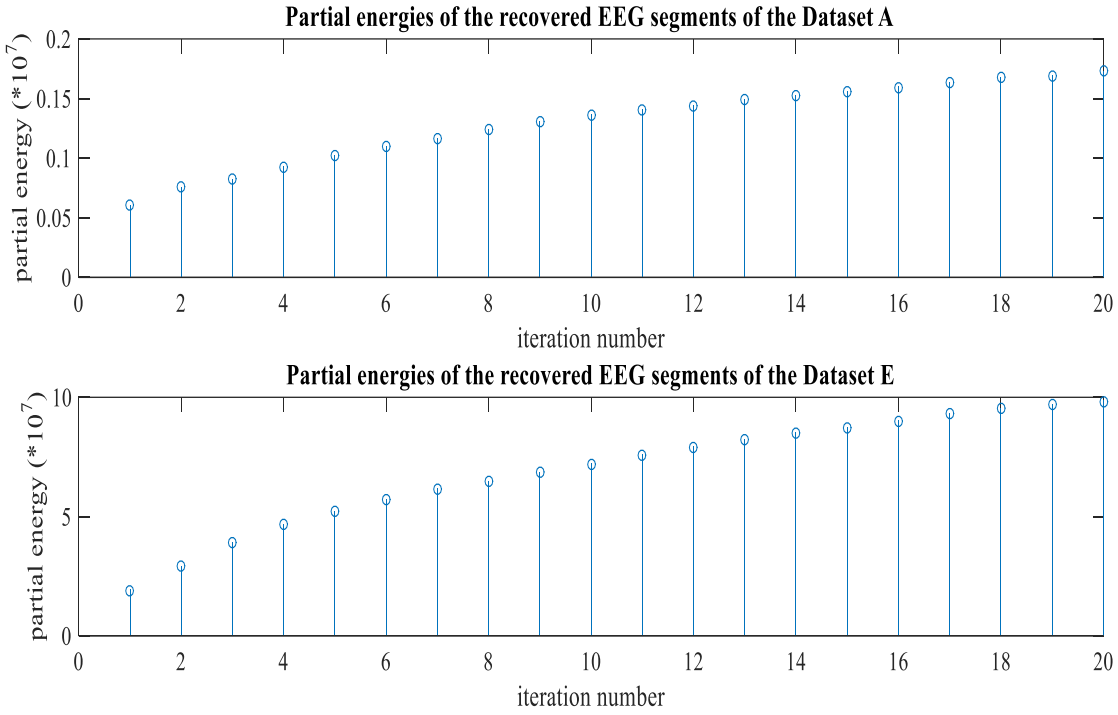

Figure 4. The distribution of the partial energy of the estimated EEG segments chosen from (**top**) Dataset A and (**bottom**) Dataset E, obtained at different iterations of the OMP algorithm ($P = 20$). The OMP algorithm is applied to the compressive measurements and the energy of the recovered part of the signal at each iteration is calculated and recorded.

It is observed that although, as expected, in both plots the partial energies of the recovered EEG segments increase as the number of iteration of the OMP algorithm increases, the rate by which the partial energies are increased for the seizure segment (chosen from the Dataset E) is much higher compared to that of the non-seizure segment (chosen from the Dataset A). Specifically, as observed in Figure 4, the difference between partial energies at the 5th and the 1st iterations of the OMP algorithm applied to the compressively sensed seizure and non-seizure segments are $3.3 * 10^7$and $0.042 * 10^7$, respectively. These findings are consistent for all non-seizure segments in datasets B, C, and D. Based on these results, the rate of change in the partial energy of the estimated signals obtained at different iteration of the OMP algorithm applied to the compressed EEG measurements is used in this study as a new feature for discriminating seizure segments from non-seizures. Based on its definition, the proposed feature is called the partial energy difference (PED).

In the proposed method, at the 1st step, the OMP algorithm (detailed in Algorithm 1) is run with input arguments $\mathbf{y}$ (the compressive measurements), $\mathbf{\Phi}$ (the random sparse binary sensing matrix), $\mathbf{\Psi}$ (the DCT sparsifying matrix), and the sparsity level (number of iterations) $K = 1$. The output of this step is the estimated signal $\hat{\boldsymbol{x}}_1$:

$$\hat{\boldsymbol{x}}_1 = [\hat{x}_1, \hat{x}_2, \dots, \hat{x}_N]^T. \tag{13}$$

The energy of this estimated signal is calculated and stored in the variable E_1 given by:

$$E_1 = \sum_{i=1}^{N} \hat{x}_i{}^2. \tag{14}$$

The above procedure is repeated for K = b. The output of this step is the estimated vector $\hat{\boldsymbol{x}}_b$ with energy E_b. The feature used in the proposed method is given by:

$$e = E_b - E_1. \tag{15}$$

The parameter b is key in controlling the trade-off between the seizure detection performance and the execution time (computational complexity) of the proposed approach. The value of this parameter b is found by taking into account the following points:

1. It is data-dependent and its value should be found by analyzing few EEG segments of the database under analysis.

2. The value of this parameter varies between 2 and b_{max}, where b_{max} is equal to the sparsity level of the signal in the transformed domain. For the non-sparse signals, b_{max} is equal to the epoch length (N); however, for signals such as EEGs, as shown later, the value of b_{max} is much less than the epoch length.

3. A large value of b leads to higher seizure detection performance but longer execution time and vice versa.

4. In a trade-off between detection performance and execution time, the lowest value of b after which the classification performance dose not significantly increases is chosen. As an example, the classification results for different values of this parameter for the {C}-{E} classification experiment for compression ratio of 0.05 and epoch length of 256 samples are given in Table 3. The classification performance of the PED is measured using the area under the receiver operating characteristic curve (AUC). It should be noted that these results are obtained from analyzing a small subset of the datasets. The results show that for $b > 5$, the AUC values do not significantly increase. The results also show that even for the minimum value of b, i.e. $b = 2$, an acceptable AUC value is achieved.

For the analysis of the Bonn University database, using similar results described in Table 3, the value of the parameter b was chosen to be 5. It should be noted that this selection was based the trade-off between accuracy and computation time by analyzing the limited EEG segments from {C}-{E} classification problem as an example—without any optimization procedure—and used for all the other experiments, not knowing if this value is optimum for these datasets. Algorithm 2 describes our proposed single-channel OMP-based algorithm for automatic epileptic seizure classification in a CS-based WBAN.

Table 3. Classification performance of the PED feature for different values of parameter b for the binary classification problem {C}-{E} for the epoch length of 256 samples (1.47 seconds) and for the compression ratio of 0.05. Execution times are given in seconds. The AUC is used as a measure of the classification performance.

b	AUC	Exe. time (S)
2	0.926	0.8
3	0.954	1.0
4	0.962	1.0
5	0.964	1.2
6	0.965	1.3
7	0.966	1.5
8	0.966	1.6

Algorithm 2. Epileptic seizure classification based on orthogonal matching pursuit algorithm (the proposed method).

Inputs:

- One compressed EEG epoch
- Parameter b

Outputs:

- Feature value

Procedure:

1. Initialize the averaging variable $\mathrm{V} = 100$[۳].
2. Define a vector $\mathbf{E}$ of length V. Let $\mathbf{E} = \mathbf{0}$.
3. Define the iteration counter v. Let $\mathrm{v} = 1$.
4. Generate the random binary sensing matrix $\boldsymbol{\Phi}$ with the parameter $\mathrm{d} = 2$.
5. Run the OMP algorithm with the input arguments $\mathbf{y}$, $\boldsymbol{\Phi}$, $\boldsymbol{\Psi}$, $\mathrm{K} = 1$.
6. Calculate the energy of the estimated signal obtained from the Step 5 and store them in variable E_1.
7. Run the OMP algorithm with the input arguments $\mathbf{y}$, $\boldsymbol{\Phi}$, $\boldsymbol{\Psi}$, $\mathrm{K} = \mathrm{b}$.
8. Calculate the energy of the estimated signal obtained from the Step 7 and store them in variable E_b.
9. Calculate the energy difference (our proposed feature) $\mathrm{e} = \mathrm{E}_\mathrm{b} - \mathrm{E}_1$ and store it in the vector $\boldsymbol{E}$ according to $\mathbf{E}(\mathrm{v}) = \mathrm{e}$.
10. Increment the parameter v by 1.
11. If v is less than $\mathrm{V} + 1$, go to Step 4.
12. Calculate the average of the vector $\mathbf{E}$ as e_avg and return it as feature value.

It is worth emphasizing that, as depicted in Figure 3, the main difference between the proposed and existing methods is in the reconstruction block at the server node. While existing approaches need full reconstruction of EEG samples, the proposed method uses only partial reconstructed ones by choosing a small value for the parameter b. In summary, the main contributions of this proposed approach are as follows:

1. Existing methods in CS-based WBANs require full reconstruction of EEG samples at the server nodes. Full reconstruction of original EEG signals from their compressive measurements is a time-consuming procedure and not suitable for real-time EEG applications.

[۳] Note that due to the randomness of the sensing matrix $\boldsymbol{\Phi}$, the algorithm is run for many sensing matrices.

2. The proposed method, when applied to both single-channel and multichannel EEG databases, can achieve large AUC values with very small execution times.

3. The proposed feature paves the way for the development of an accurate detection method with very low execution time which can be run on a mobile device to give real-time feedback to the patient or doctor before transmission.

In order to compare the performance of the PED feature with that of the MD feature reported in (Raghu et al., 2019), the performance of the proposed method was evaluated for 4 different classification problems: {A}-{E}, {B}-{E}, {C}-{E}, and {D}-{E}using the AUC. Also, as explained in Section 2.3, before applying the MD classification algorithm, the compressive measurements were fully reconstructed using the BSBL algorithm. The performance of the algorithms was compared using both the AUC and execution time. It should be emphasized that the selection of the MD algorithm as the benchmark in the single-channel case was based on fact that the experimental results reported in (Raghu et al., 2019) show that this method outperforms the state-of-the-art methods in terms of the seizure detection performance as well as the execution time.

2.4.2. Multivariate version of the proposed method

The proposed single-channel seizure detection methodology described in Section 2.4.1 is extended to multichannel signals by:

1. Substituting the OMP algorithm with its multivariate counterpart, i.e., SOMP that can recover all original EEG signals from their compressive measurements simultaneously. This algorithm assumes the row-sparsity assumption for the EEG signals in the sparsifying domain. Algorithm 3 describes the different steps of this algorithm. More details about this algorithm can be found in (Joel A. Tropp et al., 2006).
2. Substituting the norm-2 (energy operator) with the Frobenius norm to calculate the multivariate feature for seizure detection in multichannel EEGs.

So, the multivariate form of the proposed feature in (15) is defined as:

$$E = \left\|\widehat{\boldsymbol{X}}_{\boldsymbol{b}}\right\|_F^2 - \left\|\widehat{\boldsymbol{X}}_{\boldsymbol{1}}\right\|_F^2, \tag{16}$$

where $\widehat{\boldsymbol{X}}_{\boldsymbol{1}}$ and $\widehat{\boldsymbol{X}}_{\boldsymbol{b}}$ are the reconstructed matrices by running the SOMP algorithm for 1 and b iteration respectively, and $\|.\|_F$ is the Frobenius norm defined in (8). In (16), the parameter b represents the row-sparsity level of the EEG matrix and its value varies between 2 to N(epoch length). For the analysis of the CHB-MIT database, similar to the procedure used for the selection of b for the Bonn database, the results obtained from analyzing 3 segments randomly selected from the subjects 01 and 03 were used. Then, in a trade-off between the classification performance and the execution time, the value of this parameter was chosen to be 15 as the experimental results show that further increasing this value leads to the higher execution time and does not significantly increase the classification performance. This value is used for analyzing all the other selected subjects of the CHB-MIT database. For each subject, the values of the feature were calculated for successive epochs of length 3 seconds, i.e. 768 samples, and 2 seconds overlaps. In total, 298 seizure epochs and 298 non-seizure epochs from each subject were analyzed.

Algorithm 3. The simultaneous orthogonal matching pursuit algorithm.

Inputs:

- An M × CH measurement matrix $\boldsymbol{Y}$
- An M × N sensing matrix $\boldsymbol{\Phi}$
- An N × N sparsifying matrix $\boldsymbol{\Psi}$
- The row-sparsity level K of the original signal matrix $\boldsymbol{X}$

Output:

- The estimated N × CH signal matrix $\widehat{\mathbf{X}}$

Procedure:

1. Initialize the residual $\mathbf{R_0} = \mathbf{Y}$, the estimated signal $\widehat{\mathbf{X}}_\mathbf{0} = \mathbf{0}$, the index set $\Omega_0 = \emptyset$, the iteration counter $\mathrm{t} = 1$, and the N × 1 transform domain coefficient vector $\widehat{\boldsymbol{W}} = \mathbf{0}$.
2. Calculate the new matrix $\mathbf{A} = \boldsymbol{\Phi}\boldsymbol{\Psi}'$ where $\boldsymbol{\Psi}'$ is the transpose of the matrix $\boldsymbol{\Psi}$.
3. Compute the $N \times CH$ correlation matrix $\boldsymbol{C}$ according to: $\boldsymbol{C} = \left|\acute{\boldsymbol{A}}\boldsymbol{R_{t-1}}\right|$.
4. Compute the $N \times 1$ vector $\boldsymbol{c}$ by: $\boldsymbol{c} = vecnorm(\boldsymbol{C})$. Note that $vecnorm(\boldsymbol{C})$ calculate the 2 norm of each row of matrix $\boldsymbol{C}$.
5. Find the index λ_t that correspond to the position of the maximum of the vector $\boldsymbol{c}$.
6. Update the index set: $\Omega_\mathrm{t} = \Omega_{\mathrm{t}-1} \cup \{\lambda_\mathrm{t}\}$.
7. Update the coefficients: $\mathbf{X1_t} = \mathbf{A}_{\Omega_\mathrm{t}}^{\dagger}\mathbf{Y}$ where $\mathbf{B}^{\dagger}$ represents the pseudo inverse of the matrix $\mathbf{B}$ and $\boldsymbol{B}_\Omega$ represents the columns of $\boldsymbol{B}$ that Ω shows. .
8. Update the residual: $\mathbf{R_t} = \mathbf{Y} - \mathbf{A}_{\Omega_\mathrm{t}}\mathbf{X1_t}$.
9. Increment the iteration counter by 1: $\mathrm{t} = \mathrm{t} + 1$.
10. If t is less than $\mathrm{K} + 1$, go to Step 3.
11. Update the transform domain coefficient vector: $\widehat{\mathbf{W}}_\mathbf{\Omega} = \mathbf{X1_t}$.
12. Calculate the estimated signal: $\widehat{\mathbf{X}} = \boldsymbol{\Psi}'\widehat{\mathbf{W}}$.

2.5. Threshold-based classification using the PED feature

We used a binary classifier which simply compared the value of the PED feature extracted from the input (multichannel or single-channel) EEG signal with a threshold γ to classify the EEG as seizure or non-seizure. The value of the threshold γ was obtained through training in which the ROC analysis was performed on the train data and the threshold value for which the sensitivity was equal to 0.9 was found. The performance of the binary classifier based on the selected threshold was evaluated using the leave-one-out cross-validation (LOO-CV) procedure applied to the 10 selected EEG datasets (corresponding to 10 different subjects) of the CHB-MIT database.

2.6. Performance evaluation

Performance of the proposed PED feature was assessed using AUC, accuracy, sensitivity, and specificity. All the experiments were implemented using MATLAB R2015a and run on a laptop with 16 GB RAM and a 2.7 GHz Core i7-7500U Intel CPU.

3. Results and discussion

As mentioned earlier, choosing a small value for the parameter d, i.e. the number of 1s in each of the columns of the random binary sensing matrix, significantly reduces the computational loads of the WBAN system, which in turn would lead to less battery capacity at the sensor nodes. Therefore, the value of this parameter should be chosen as

small as possible. Experimental results show that the recovery algorithms, i.e. OMP and SOMP, performed poorly when the value was set to 1; so in all experiments performed in this study the value of the parameter d was set to 2. Also, as previously explained, the parameter b, i.e. the sparsity level in the OMP algorithm and the row-sparsity level in the SOMP algorithm, was set to 5 and 15 in the analysis of single-channel and the multichannel databases, respectively.

3.1. Results of the analysis of the Bonn University database using the PED feature

Figure 5 shows the distribution of the PED values for all the EEG segments of length 1024 samples (5.89 seconds) in the 5 EEG datasets A, B, C, D, and E, compressively sensed at the CR of 0.05. It clearly shows that: 1) the PED values for seizure (Dataset E) and non-seizure (datasets A to D) segments are different, and 2) the PED values for seizure segments are higher than those of non-seizures segments. Therefore, the PED can be used to successfully classify seizure and non-seizure segments.

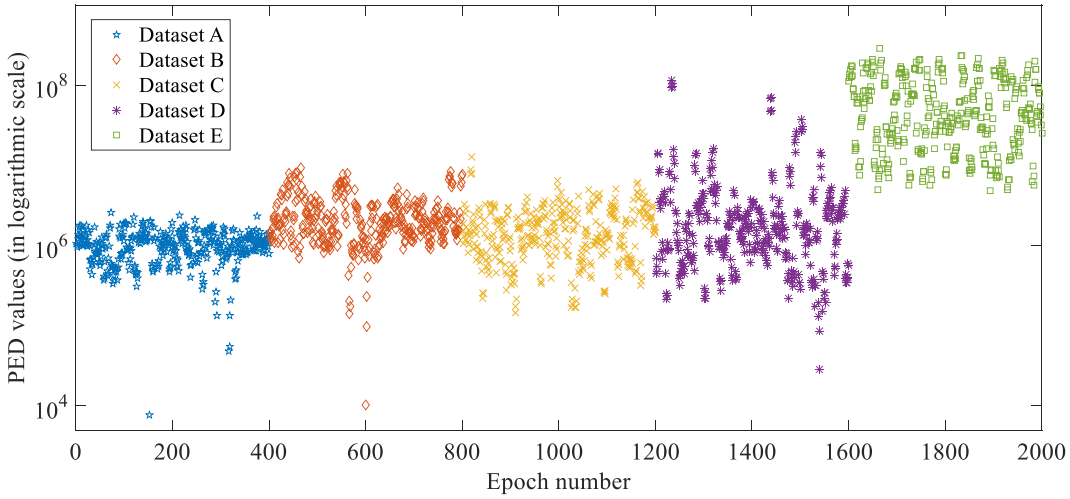

Figure 5. The distribution of the values of the univariate PED feature in (15) for the datasets A, B, C, D, and E, for epoch length of 1024 samples (5.89 seconds) and compression rate (CR) of 0.05. Dataset E consists of seizures; the other datasets are seizure free.

Figures 6-8 shows the box plots of the values of the univariate version of the PED feature given in (15) extracted from all the EEG segments of lengths 256 and 1024 samples (corresponding to 1.47 and 5.89 seconds lengths) in the 5 EEG datasets A, B, C, D, and E, compressively measured at 3 different CRs, i.e., 0.05 (Figure 6), 0.1 (Figure 7), and 0.2 (Figure 8). It should be noted that since the segment length in the MD algorithm should be a complete square number, segments of lengths 256 and 1024 samples were chosen. Note that, for example, for CR=0.05 and segment length of 256 samples, only 12 samples randomly selected from the EEG segment under analysis is used to extract the PED feature. It should be also noted that the CR of 0.05 has been rarely used in the field of CS of EEG signals. This is because there is no reconstruction algorithm that can recover the EEG signals from their compressive measurements in this rate with an acceptable NMSE. Therefore, it would not be possible to use existing EEG analysis techniques which require full reconstruction of the compressive measurements. The box plots show that the values of the proposed feature for the EEG segments in the Dataset E are considerably greater than the values for the EEG segments in all the other 4 datasets. The plots also show that the PED values increase as the length of the EEG epochs increases. The

plots therefore show the ability of the proposed PED feature in differentiating between seizure and non-seizure segments. These findings are supported by the AUC results in Tables 4 and 5.

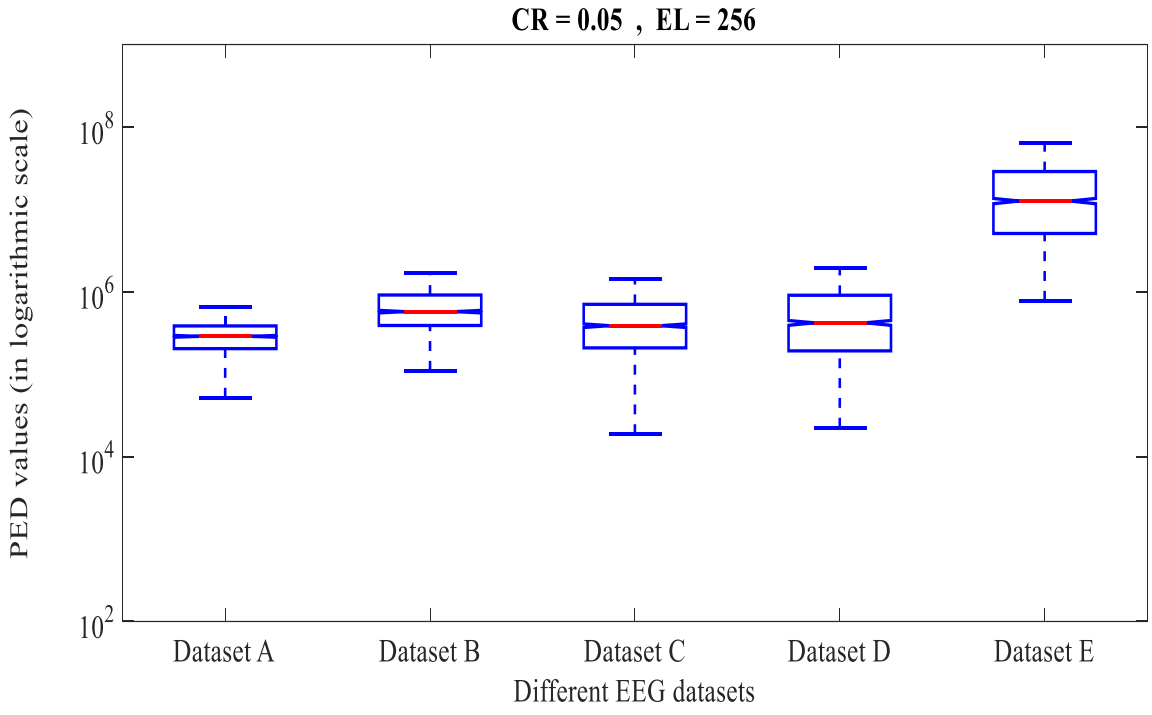

(a)

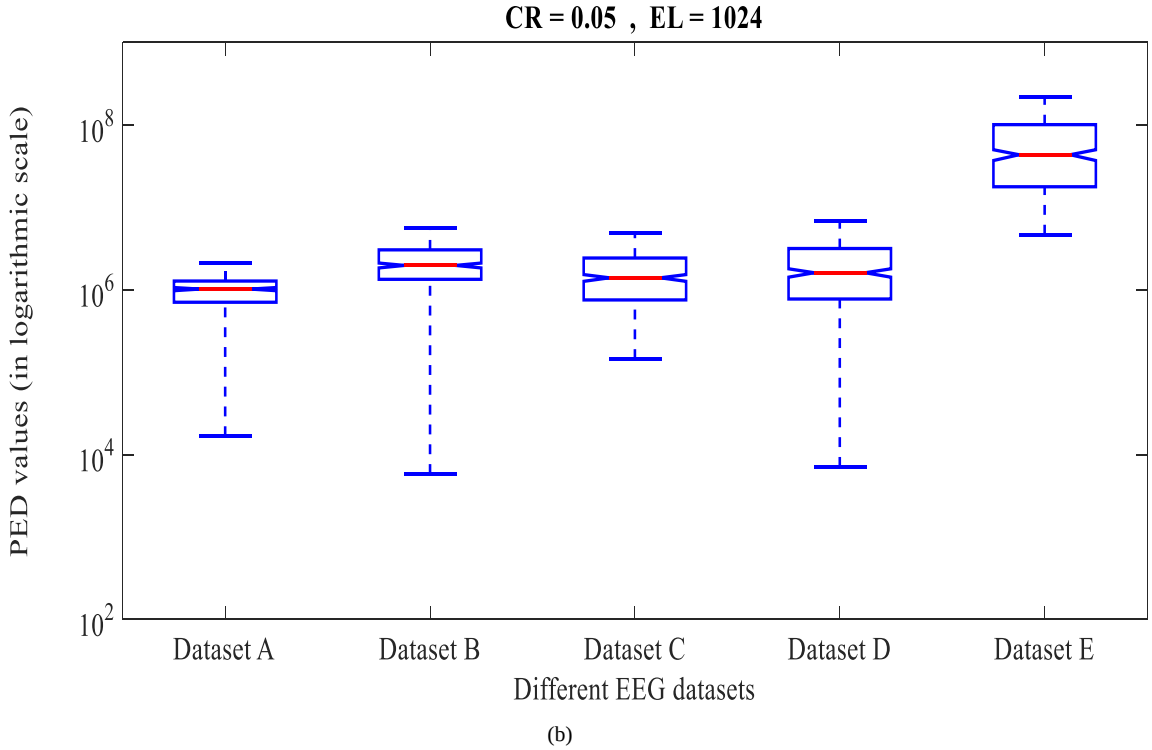

(b)

Figure 6. Box plots showing the values of the proposed single-channel PED feature in (15) for the datasets A, B, C, D, and E for 2 epoch lengths (ELs) and compression rates (CR) of 0.05. (a) $EL = 256$. (b) $EL = 1024$.

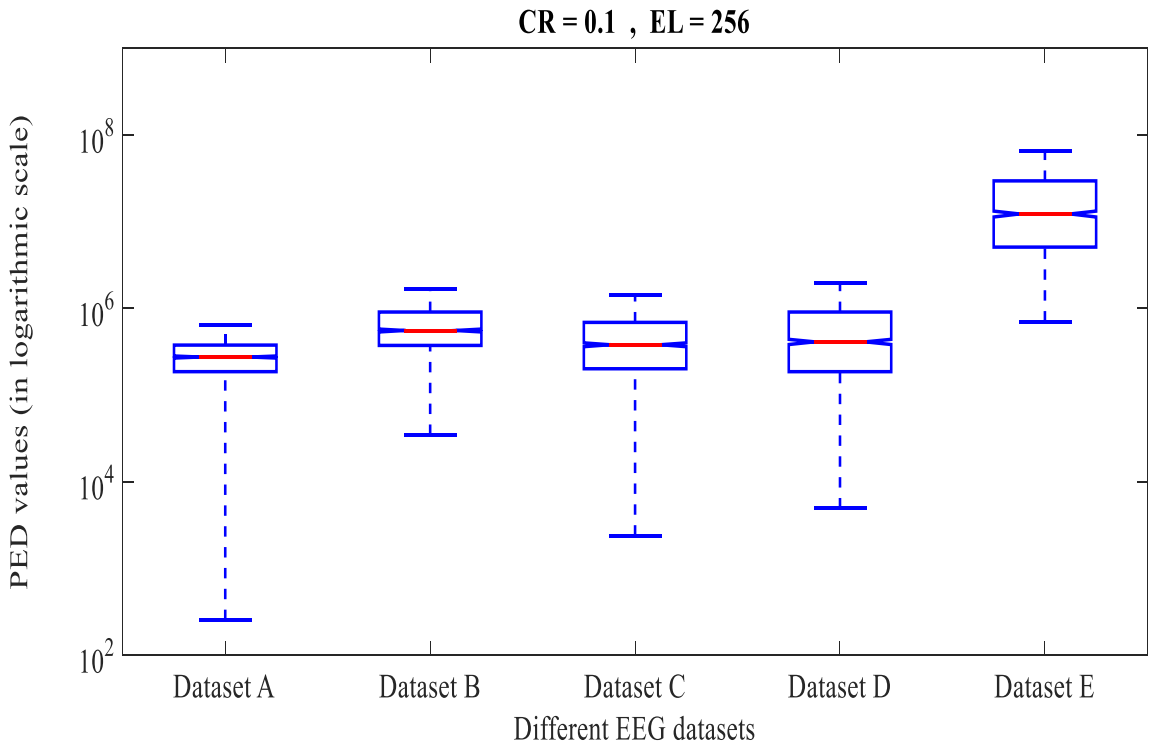

(a)

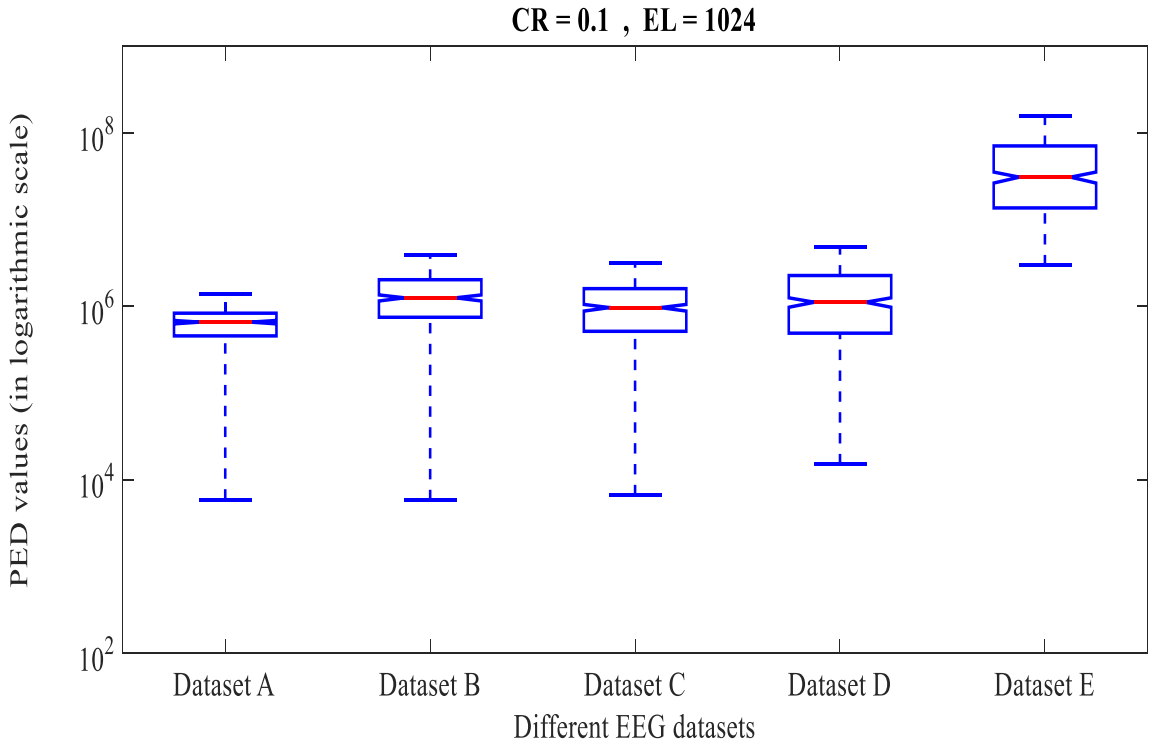

(b)

Figure 7. Box plots showing the values of the proposed single-channel PED feature in (15) for the datasets A, B, C, D, and E for 2 epoch lengths (ELs) and compression rates (CR) of 0.1. (a) $EL = 256$. (b) $EL = 1024$.

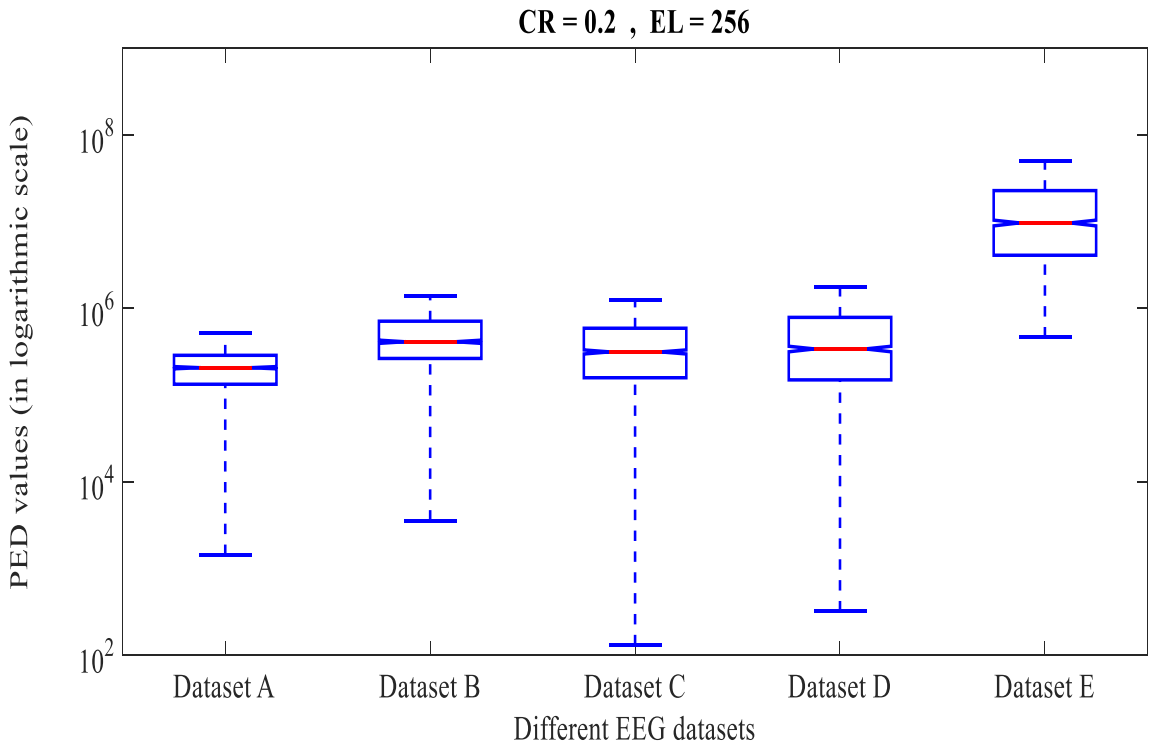

(a)

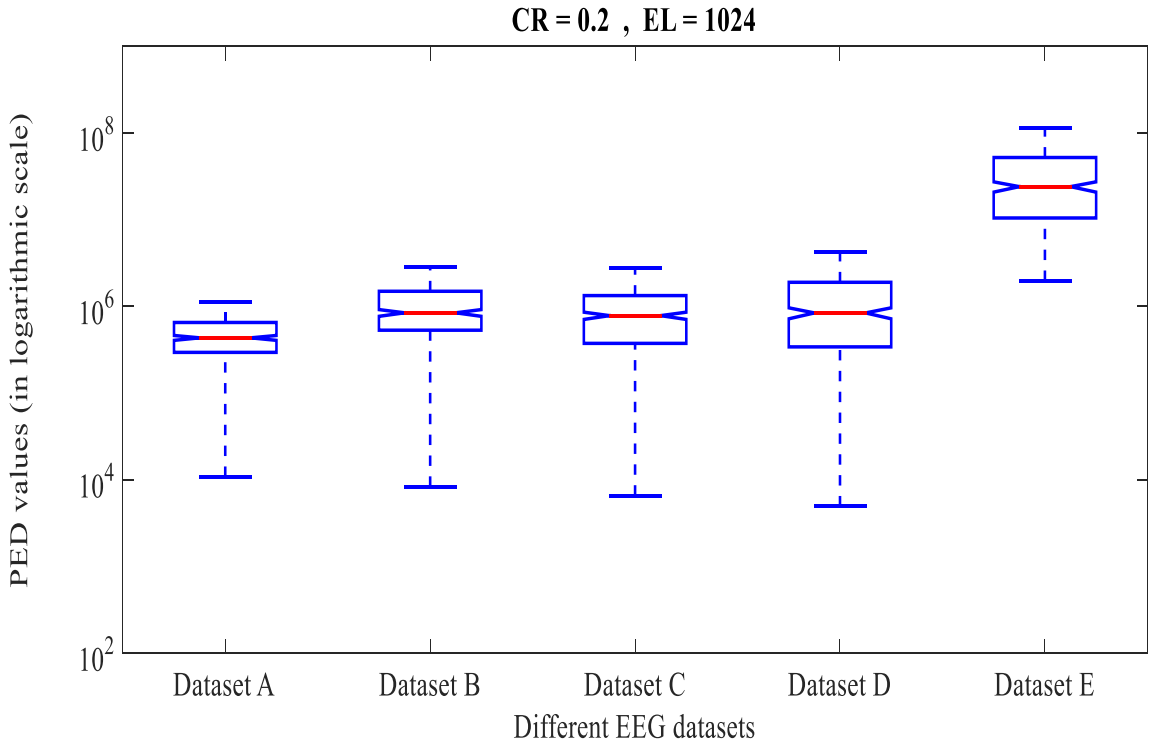

(b)

Figure 8. Box plots showing the values of the proposed single-channel PED feature in (15) for the datasets A, B, C, D, and E for 2 epoch lengths (ELs) and compression rates (CR) of 0.2. (a) $EL = 256$. (b) $EL = 1024$.

Table 4 shows the performance of the PED feature in comparison with the MD algorithm for the epoch length of 256 samples, for the classification problems {A}-{E}, {B}-{E}, {C}-{E}, and {D}-{E} and for 3 values of CR. At this epoch length when the CR is 0.05, it is not possible to reconstruct the EEGs from compressive measurements and therefore the MD algorithm is not applicable (N/A) here. Similar results with epoch length of 1024 samples are reported in Table 5. We observe that: 1) the proposed PED feature outperforms the MD algorithm in terms of the values of the AUCs in the classification problems {A}-{E}, {B}-{E}, and {C}-{E} for all the 3 CRs and for the 2 epoch lengths, 2) in terms of the execution time, the proposed feature is by far superior to the MD algorithm in all classification problems and for all CRs, 3) in the {D}-{E} classification problem for the epoch length of 256 samples, the MD algorithm performs better than the proposed feature in terms of the values of the AUCs; however, the execution time for the proposed method is still much lower, and 4) the proposed method outperforms the MD algorithm at lower CRs.

Table 4. Classification results for the binary classification problems {A}-{E}, {B}-{E}, {C}-{E}, and {D}-{E} for the epoch length of 256 samples (1.47 seconds). Execution times are given in seconds. N/A: not applicable; MD: matrix determinant.

Classification problem	Algorithm	CR=0.05		CR=0.1		CR=0.2	
		AUC	Exe. time (S)	AUC	Exe. time (S)	AUC	Exe. time (S)
{A}-{E}	MD	N/A	N/A	0.969	1647	0.985	1904
	PED (proposed)	0.973	1.1	0.985	1.3	0.991	1.5
{B}-{E}	MD	N/A	N/A	0.931	2006	0.957	1900
	PED (proposed)	0.957	1.1	0.970	1.4	0.974	1.5
{C}-{E}	MD	N/A	N/A	0.968	1954	0.986	1909
	PED (proposed)	0.964	1.1	0.977	1.4	0.981	1.5
{D}-{E}	MD	N/A	N/A	0.949	1626	0.974	1839
	PED (proposed)	0.938	1.1	0.948	1.3	0.950	1.5

Table 5. Classification results for the binary classification problems {A}-{E}, {B}-{E}, {C}-{E}, and {D}-{E} for the epoch length of 1024 (5.89 seconds). Execution times are given in seconds. MD: matrix determinant.

Classification problem	Algorithm	CR=0.05		CR=0.1		CR=0.2	
		AUC	Exe. time (S)	AUC	Exe. time (S)	AUC	Exe. time (S)
{A}-{E}	MD	0.987	2552	0.988	2793	0.997	5252
	PED (proposed)	0.998	4.1	0.999	5.8	0.999	8.9
{B}-{E}	MD	0.963	2415	0.979	2855	0.979	5309
	PED (proposed)	0.988	4.3	0.982	5.8	0.988	8.8
{C}-{E}	MD	0.980	2380	0.989	2995	0.994	5393
	PED (proposed)	0.993	4.1	0.995	5.4	0.993	8.5
{D}-{E}	MD	0.958	2575	0.974	2978	0.983	5317
	PED (proposed)	0.964	5.0	0.965	5.5	0.961	8.5

3.2. Results of the analysis of the CHB-MIT database using the PED feature

Figure 9 shows the distribution of the PED values for all the EEG segments of length 768 samples (3 seconds sliding windows with 2 seconds overlap) of the Subject 01 of the CHB-MIT database, compressively sensed at the CR of 0.05. It demonstrates a good discrimination between seizure and non-seizure segments. In Figure 9, the PED values for seizure segments are clearly higher than non-seizure segments. This shows that the multivariate PED feature can be used to classify seizure and non-seizure segments in multichannel EEG signals.

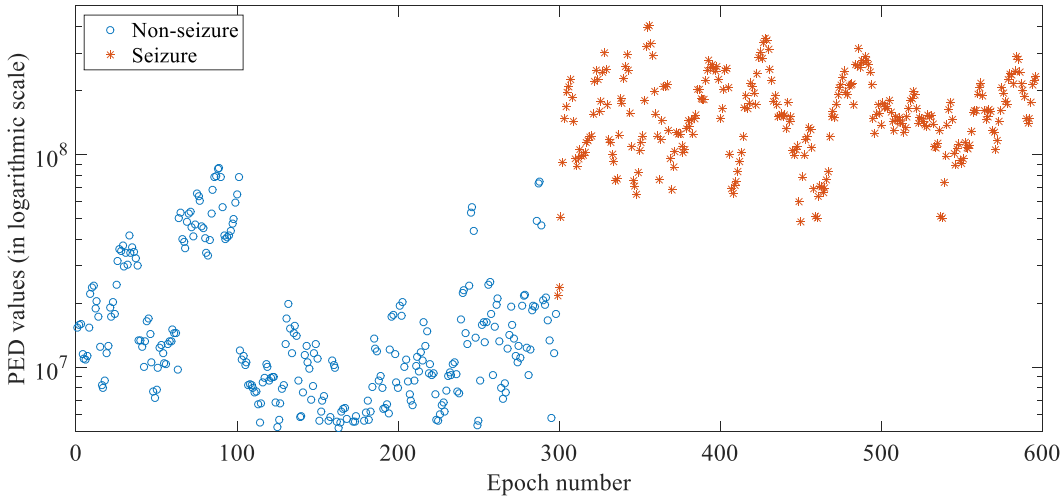

Figure 9. The distribution of the values of the multivariate PED feature in (16) extracted from the multichannel EEG segments of length 768 samples (3 seconds sliding windows with 2 seconds overlap) of the Subject 01 compressively sensed at the compression ratio of 0.05.

The performance of the proposed multivariate feature given in (16) was evaluated using the CHB-MIT multichannel database. For illustration, Figure 10 shows the boxplots of the values of the proposed feature for Subject 01 at 3 CR values of 0.05, 0.1, and 0.2. The results show that the values of the proposed multivariate feature for the seizure segments are much larger than the values for non-seizure segments for all CRs with little overlap, indicating the utility of the proposed multivariate feature as a good biomarker of seizure in multichannel EEGs. It should be noted that these findings are consistent for all the selected subjects from the CHB-MIT database.

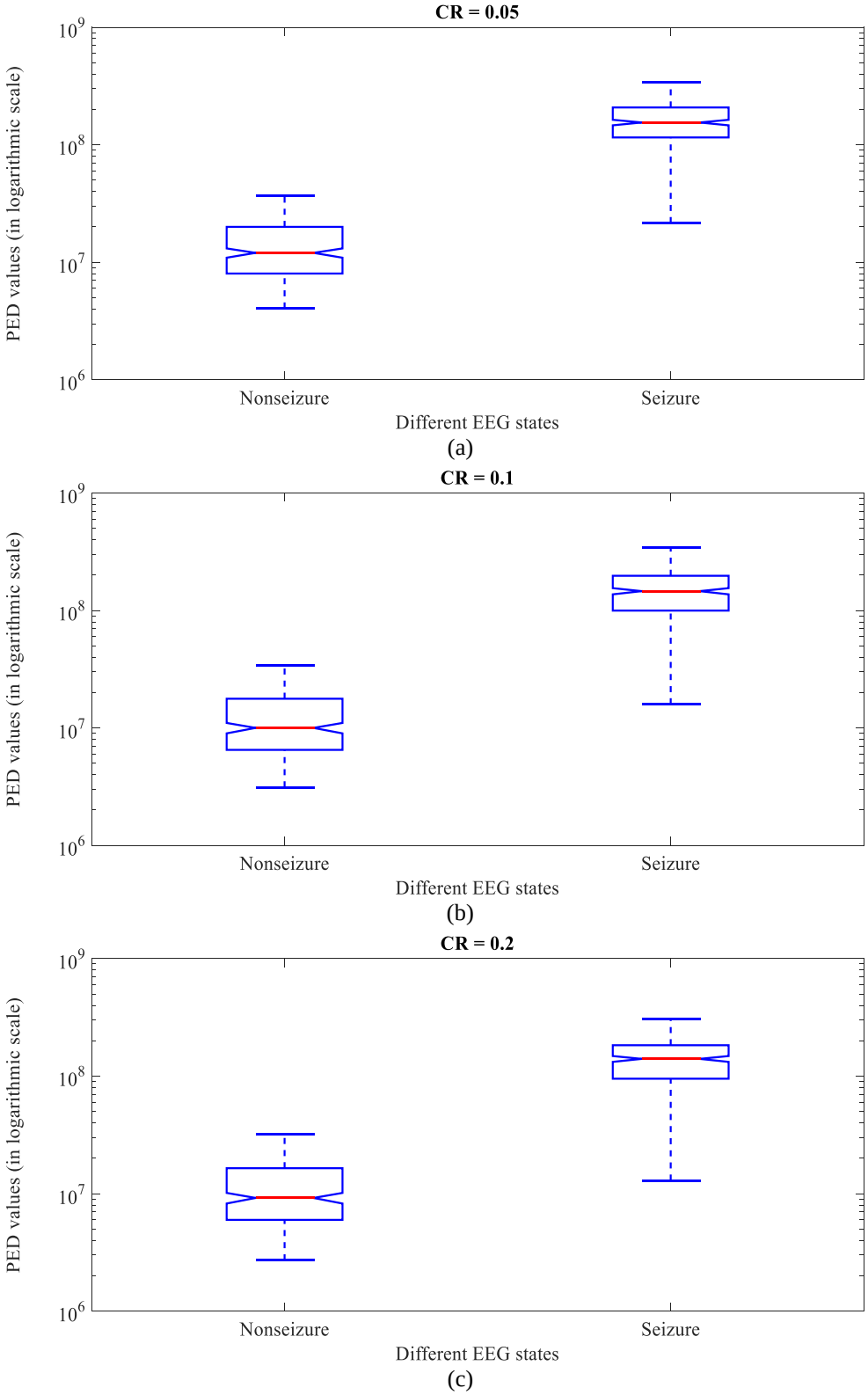

Figure 10. Box plots showing the values of the proposed multivariate feature in (16) extracted from the EEG segments of length 768 (3 seconds sliding windows with 2 seconds overlap) of the Subject 01 compressively measured at 3 different CRs of (a) $CR = 0.05$. (b) $CR = 0.1$. and (c) $CR = 0.2$.

Table 6 shows the performance of the proposed feature for all the selected subjects of the CHB-MIT database. The results show that, for all the 3 CRs, the proposed feature achieves high AUC values with low execution time.

Table 6. The AUC values and the execution times of the multivariate PED feature for different subjects of the CHB-MIT database. Execution times are given in seconds.

Subject ID	CR=0.05		CR=0.1		CR=0.2	
	AUC	Exe. time (S)	AUC	Exe. time (S)	AUC	Exe. time (S)
Subject 01	0.993	9.9	0.992	11.2	0.991	13.9
Subject 03	0.932	9.4	0.929	10.6	0.926	13.3
Subject 04	0.887	9.5	0.900	11.3	0.907	14.6
Subject 05	0.994	9.6	0.994	10.8	0.992	12.8
Subject 07	0.990	9.4	0.988	10.5	0.985	13.0
Subject 08	0.921	9.8	0.926	10.6	0.927	12.8
Subject 10	0.974	9.4	0.972	10.8	0.963	13.0
Subject 11	0.929	9.3	0.921	10.7	0.919	13.0
Subject 18	0.845	9.4	0.844	10.6	0.842	12.6
Subject 23	0.953	9.3	0.950	10.6	0.945	12.9
Mean	0.941	9.5	0.941	10.7	0.939	13.1

There are many high-performance seizure detection algorithms in the literature that use feature-based and/or deep learning and time-frequency methods, e.g. (Bhattacharyya & Pachori, 2017; Hossain et al., 2019; Kaleem et al., 2018; Zabihi M Fau - Kiranyaz et al., 2020). In (Bhattacharyya & Pachori, 2017), a novel time-frequency method using multivariate extension of empirical wavelet transform is presented for the seizure detection from the multichannel EEG signals. This approach was applied to the CHB-MIT database and an average accuracy of 0.994 was achieved. In (Hossain et al., 2019) a deep learning methodology is presented for seizure detection which extracts spectral and temporal features from raw EEGs to train a convolutional neural network to the general structure of seizure events. The results of applying this method on the CHB-MIT database shows that it exhibits a total accuracy of 0.980 in a cross-patient seizure detection scenario. The patient-specific seizure detection methodology presented in (Kaleem et al., 2018) is based on signal-derived EMD-based dictionary approach and achieves the average AUC value of 0.960 for the CHB-MIT database. In (Zabihi M Fau - Kiranyaz et al., 2020), a method is presented that characterizes the dynamic behavior of seizure events by Nullcline analysis in the phase space. The results show that this method can achieve the average AUC value of 0.931 for the CHB-MIT database. However, unlike the univariate proposed feature, there is no single multivariate feature in the literature for detecting seizures in multichannel EEGs, so we could compare the performance of the proposed multivariate feature with it. On the other hand, comparing the performance of the proposed multivariate feature with existing methodologies which use combination of features from different domain with optimized pre– and post-processing algorithms would not be fair. However, as mentioned previously, all the existing methods for detecting seizures in multichannel EEGs in WBAN-based systems require reconstruction of the original EEG data from their compressive measurements. To give an idea as to how long this reconstruction may take and what the resulted NMSE could be, as an example, we recovered 10 minutes of multichannel EEG of Subject

01 from their compressive measurements using the row-sparse multiple measurement vector (RSMMV) recovery algorithm presented in (Shukla & Majumdar, 2015). This algorithm was chosen because it is relatively fast and can recover original EEG signals with lower NMSEs compared to the SOMP algorithm. It should be noted that, despite its high recovery performance, the RSMMV algorithm is not applicable in the implementation of the proposed feature because: 1) it is not a greedy iterative recovery algorithm, and 2) it has a high execution time than the OMP/SOMP algorithms so is not suitable for real-time applications. The execution time and NMSE of the RSMMV algorithm applied to 10 minutes of multichannel EEGs of Subject 01 for 3 CRs are given in Table 7. The results show that the NMSEs for the reconstructed signals are high especially for low CRs, e.g. NMSE=0.956 at CR=0.05. This means that existing high-performance multichannel seizure detection methods may fail for such CRs. The results also show that as CR increases, although the NMSE decreases, the computational time required for signal recovery increases significantly. Thus, existing multichannel seizure detection methods may not be suitable for real-time seizure detection in WBANs when the CR is very low.

Table 7. The values of the NMSE and the execution time of the RSMMV recovery algorithm when used to reconstruct 10 minutes of multichannel EEGs of the Subject 01 of the CHB-MIT database. The results are given for 3 different CRs.

CR	NMSE	Exe. time (S)
0.05	0.956	604.6
0.1	0.884	656.1
0.2	0.701	671.7

In summary, these experimental results highlight the suitability of the proposed feature for real-time WBAN-based automatic seizure detection systems at low CRs. It is worth mentioning that there are some high-performing seizure detection techniques which use lower sampling frequencies, such as 32 Hz, e.g. (O'Shea, Lightbody, Boylan, & Temko, 2020). For the databases used in this study, this is approximately equivalent to the CR of 0.2 which is still much higher than the CRs of 0.05 and 0.1 for which the proposed method performs well. In addition, such techniques need anti-aliasing filters before down-sampling which is not easy (in terms of computational load) to be implemented at the sensor nodes in WBANs.

Table 8 shows the average performance of the LOO-CV testing results for the PED-based classifier. The results show that: 1) the proposed PED feature performs well when used for classifying seizure and non-seizure segments in a real multichannel EEG database, and 2) the performance of the PED feature is not subject-dependent. It should be emphasized that this performance was obtained by using only a single feature, i.e. the PED, and the simplest classifier, i.e. the threshold-based binary classifier. These together with the fact that the classification is performed on compressively sensed multichannel signals without executing any preprocessing, prove the effectiveness of the feature for the purpose of seizure classification in WBAN systems. It should also be emphasized that we have specifically avoided using a feature-based machine learning approach, or even a deep learning approach, because of the

computational complexity as this would have conflicted with the over-arching goal of our approach to keep computational low so the method can be applicable to WBAN systems.

Table 8. The average values of the sensitivity, specificity, and accuracy obtained from the leave-one-out cross-validation (LOO-CV) testing of the PED-based classifier. Epochs were of length 768 samples (3 seconds sliding windows with 2 seconds overlap), extracted from the 10 selected subjects of the CHB-MIT database, compressively sensed at the 3 compression ratios of 0.05, 0.1, and 0.2. Mean AUCs are also reported.

Metric	CR=0.05	CR=0.1	CR=0.2
Sensitivity	0.873	0.872	0.871
Specificity	0.710	0.687	0.668
Accuracy	0.791	0.778	0.770
AUC	0.914	0.909	0.904

4. Conclusions and future work

Existing automatic epileptic seizure detection methods, if to be used in CS-based WBAN systems, need the reconstruction of full EEG samples from their compressive measurements. In CS frameworks, reconstruction is a time-consuming and computationally expensive procedure that it is not suitable for WBANs. Besides, at very low CRs, the reconstructed signals may not have the quality needed for accurate seizure detection. In order to overcome these limitations, we propose a novel real-time seizure detector, using a partial energy difference (PED). This system does not require the reconstruction of full EEG samples. The experimental results showed that, in single-channel case in comparison with the benchmark MD seizure detection algorithm, the proposed method achieves an improvement of up to 4% in AUCs when used to classify the EEG signals in the Bonn University database. Also, in terms of the execution time, the proposed method is approximately up to 3 orders of magnitude faster than the MD algorithm.

In the multichannel scenario, the proposed multivariate seizure detection method achieves AUC values ranging from 0.842 to 0.994 for 10 selected subjects in the CHB-MIT database and these results are competitive with existing methods. Also, the execution time of the proposed approach is 2 orders of magnitude less than execution time for existing WBAN seizure detection systems. The proposed methods therefore have the potential to be deployed for tele-monitoring of epilepsy patients using WBANs in personalized medicine to improve their quality of life. It could also run on a mobile device and therefore give real-time feedback to the patient or doctor before transmission.

This work is the first step in automatic seizure detection from compressive measurements without reconstructing the signal. The main limitations of this study are the small numbers of patients in the multichannel database and the short-duration and heterogeneous nature of the EEG recordings in the University of Bonn database. In the future, we aim to develop new features that can be applied to compressed and partially reconstructed measurements for further improving the proposed CS-based seizure detection methods and evaluate their performance on EEG databases with large cohorts and continuous, long-duration recordings.

Acknowledgement

This work is supported by the “Cognitive Sciences and Technologies Council” (CSTC) of Iran with grant #7104 (http://www.cogc.ir/). JMOT is supported by Science Foundation Ireland (15/SIRG/3580 and 18/TIDA/6166).

References

Abdulghani, A. M., Casson, A. J., & Rodriguez-Villegas, E. (2012). Compressive sensing scalp EEG signals: implementations and practical performance. *Medical & Biological Engineering & Computing, 50*(11), 1137-1145. doi:https://doi.org/10.1007/s11517-011-0832-1

Aghababaei, M. H., & Azemi, G. (2020). A modified row-sparse multiple measurement vector recovery algorithm for reconstructing multichannel EEG signals from compressive measurements. *Biomedical Signal Processing and Control, 60*, 101956. doi:https://doi.org/10.1016/j.bspc.2020.101956

Antonopoulos, C. P., & Voros, N. S. (2016). Resource efficient data compression algorithms for demanding, WSN based biomedical applications. *Journal of Biomedical Informatics, 59*, 1-14. doi:https://doi.org/10.1016/j.jbi.2015.10.015

Aviyente, S. (2007, 26-29 Aug. 2007). *Compressed sensing framework for EEG compression.* Paper presented at the 2007 IEEE/SP 14th Workshop on Statistical Signal Processing.

Bhati, D., Pachori, R. B., Sharma, M., & Gadre, V. M. (2020). Automated detection of seizure and nonseizure EEG signals using two band biorthogonal wavelet filter banks. In G. Naik (Ed.), *Biomedical Signal Processing: Advances in Theory, Algorithms and Applications* (pp. 137-155). Singapore: Springer Singapore.

Bhattacharyya, A., & Pachori, R. B. (2017). A multivariate approach for patient-specific EEG seizure detection using empirical wavelet transform. *IEEE Transactions on Biomedical Engineering, 64*(9), 2003-2015. doi:10.1109/TBME.2017.2650259

Candes, E. J., Romberg, J., & Tao, T. (2006). Robust uncertainty principles: Exact signal reconstruction from highly incomplete frequency information. *IEEE Transactions on Information Theory, 52*(2), 489-509. doi:https://doi.org/10.1109/TIT.2005.862083

Candes, E. J., & Tao, T. (2006). Near-optimal signal recovery from random projections: Universal encoding strategies? *IEEE Transactions on Information Theory, 52*(12), 5406-5425. doi:https://doi.org/10.1109/TIT.2006.885507

Candes, E. J., & Wakin, M. B. (2008). An introduction to compressive sampling. *IEEE Signal Processing Magazine, 25*(2), 21-30. doi:10.1109/MSP.2007.914731

Chen, S. S., Donoho, D. L., & Saunders, M. A. (1998). Atomic decomposition by basis pursuit. *SIAM Journal on Scientific Computing, 20*(1), 33-61. doi:https://doi.org/10.1137/S1064827596304010

Chiang, J., & Ward, K. R. (2014). Energy-efficient data reduction techniques for wireless seizure detection systems. *Sensors, 14*(2). doi:10.3390/s140202036

Dinesh, B., Akruti, R., Ram Bilas, P., & Vikram, M. G. (2020). Three channel wavelet filter banks with minimal time-frequency spread for classification of seizure-free and seizure EEG signals. In S. Dilip Singh, P. Ram Bilas, & G. Lalit (Eds.), *Handbook of Research on Advancements of Artificial Intelligence in Healthcare Engineering* (pp. 220-236). Hershey, PA, USA: IGI Global.

Donoho, D. L. (2006). Compressed sensing. *IEEE Transactions on Information Theory, 52*(4), 1289-1306. doi:https://doi.org/10.1109/TIT.2006.871582

Eldar, Y. C., Kuppinger, P., & Bolcskei, H. (2010). Block-sparse signals: Uncertainty relations and efficient recovery. *IEEE Transactions on Signal Processing, 58*(6), 3042-3054. doi:https://doi.org/10.1109/TSP.2010.2044837

Gilbert, A., & Indyk, P. (2010). Sparse recovery using sparse matrices. *Proceedings of the IEEE, 98*(6), 937-947. doi:10.1109/JPROC.2010.2045092

Gupta, A., Singh, P., & Karlekar, M. (2018). A novel signal modeling approach for classification of seizure and seizure-free EEG signals. *IEEE Transactions on Neural Systems and Rehabilitation Engineering, 26*(5), 925-935. doi:10.1109/TNSRE.2018.2818123

Gupta, V., Bhattacharyya, A., & Pachori, R. B. (2020). Automated identification of epileptic seizures from EEG signals using FBSE-EWT method. In G. Naik (Ed.), *Biomedical Signal Processing: Advances in Theory, Algorithms and Applications* (pp. 157-179). Singapore: Springer Singapore.

Gupta, V., & Pachori, R. B. (2019). Epileptic seizure identification using entropy of FBSE based EEG rhythms. *Biomedical Signal Processing and Control, 53*, 101569. doi:https://doi.org/10.1016/j.bspc.2019.101569

Hossain, M. S., Amin, S. U., Alsulaiman, M., & Muhammad, G. (2019). Applying deep learning for epilepsy seizure detection and brain mapping visualization. *ACM Trans. Multimedia Comput. Commun. Appl., 15*(1s), Article 10. doi:10.1145/3241056

Hussein, R., Mohamed, A., & Alghoniemy, M. (2015, 16-19 Feb. 2015). *Energy-efficient on-board processing technique for wireless epileptic seizure detection systems.* Paper presented at the 2015 International Conference on Computing, Networking and Communications (ICNC).

K.C. Santosh, S. A., D.S. Guru, and N. Dey Early detection of epileptic seizures based on scalp EEG signals. In *Medical imaging: Artificial Intelligence, Image Recognition, and Machine Learning Techniques*: CRC Press, 2019.

Kaleem, M., Gurve, D., Guergachi, A., & Krishnan, S. (2018). Patient-specific seizure detection in long-term EEG using signal-derived empirical mode decomposition (EMD)-based dictionary approach. *Journal of Neural Engineering, 15*(5), 056004. doi:10.1088/1741-2552/aaceb1

Kamal, M. H., Shoaran, M., Leblebici, Y., Schmid, A., & Vandergheynst, P. (2013, 26-31 May 2013). *Compressive multichannel cortical signal recording.* Paper presented at the 2013 IEEE International Conference on Acoustics, Speech and Signal Processing.

Majumdar, A., Shukla, A., & Ward, R. (2015, 19-24 April 2015). *Combining sparsity with rank-deficiency for energy efficient EEG sensing and transmission over Wireless Body Area Network.* Paper presented at the 2015 IEEE International Conference on Acoustics, Speech and Signal Processing (ICASSP).

Mohsina, M., & Majumdar, A. (2013). Gabor based analysis prior formulation for EEG signal reconstruction. *Biomedical Signal Processing and Control, 8*(6), 951-955. doi:https://doi.org/10.1016/j.bspc.2013.09.005

Movassaghi, S., Abolhasan, M., Lipman, J., Smith, D., & Jamalipour, A. (2014). Wireless body area networks: A survey. *IEEE Communications Surveys & Tutorials, 16*(3), 1658-1686. doi:10.1109/SURV.2013.121313.00064

Needell, D., & Tropp, J. A. (2009). CoSaMP: Iterative signal recovery from incomplete and inaccurate samples. *Applied and Computational Harmonic Analysis, 26*(3), 301-321. doi:https://doi.org/10.1016/j.acha.2008.07.002

Negra, R., Jemili, I., & Belghith, A. (2016). Wireless body area networks: Applications and technologies. *Procedia Computer Science, 83*, 1274-1281. doi:https://doi.org/10.1016/j.procs.2016.04.266

Nishad, A., & Pachori, R. B. (2020). Classification of epileptic electroencephalogram signals using tunable-Q wavelet transform based filter-bank. *Journal of Ambient Intelligence and Humanized Computing*. doi:10.1007/s12652-020-01722-8

O'Shea, A., Lightbody, G., Boylan, G., & Temko, A. (2020). Neonatal seizure detection from raw multi-channel EEG using a fully convolutional architecture. *Neural Networks, 123*, 12-25. doi:https://doi.org/10.1016/j.neunet.2019.11.023

Pawar, P., Jones, V., van Beijnum, B.-J. F., & Hermens, H. (2012). A framework for the comparison of mobile patient monitoring systems. *Journal of Biomedical Informatics, 45*(3), 544-556. doi:https://doi.org/10.1016/j.jbi.2012.02.007

Qaisar, S., Bilal, R. M., Iqbal, W., Naureen, M., & Lee, S. (2013). Compressive sensing: From theory to applications, a survey. *Journal of Communications and Networks, 15*(5), 443-456. doi:https://doi.org/10.1109/JCN.2013.000083

R. Andrzejac, K. L., F. Mormann, C. Rieke, P. David, & Elger, C. (2001). *Rev E Stat Nonlin Soft Matter Phys, 64*(6), 061907.

Raghu, S., Sriraam, N., Hegde, A. S., & Kubben, P. L. (2019). A novel approach for classification of epileptic seizures using matrix determinant. *Expert Systems with Applications, 127*, 323-341. doi:https://doi.org/10.1016/j.eswa.2019.03.021

Rahul, S., Pradip, S., & Ram Bilas, P. (2020). Automated seizure classification using deep neural network based on autoencoder. In S. Dilip Singh, P. Ram Bilas, & G. Lalit (Eds.), *Handbook of Research on Advancements of Artificial Intelligence in Healthcare Engineering* (pp. 1-19). Hershey, PA, USA: IGI Global.

Richhariya, B., & Tanveer, M. (2018). EEG signal classification using universum support vector machine. *Expert Systems with Applications, 106*, 169-182. doi:https://doi.org/10.1016/j.eswa.2018.03.053

Said, A., & Pearlman, W. A. (1996). A new, fast, and efficient image codec based on set partitioning in hierarchical trees. *IEEE Transactions on Circuits and Systems for Video Technology, 6*(3), 243-250. doi:10.1109/76.499834

Serna, J. A. d. l. O., Paternina, M. R. A., Zamora-Méndez, A., Tripathy, R. K., & Pachori, R. B. (2020). EEG-rhythm specific Taylor–Fourier filter bank implemented with O-Splines for the detection of epilepsy using EEG signals. *IEEE Sensors Journal, 20*(12), 6542-6551. doi:10.1109/JSEN.2020.2976519

Sharma, R., Sircar, P., & Pachori, R. B. (2019). Computer-aided diagnosis of epilepsy using bispectrum of EEG signals. In S. Paul (Ed.), *Application of Biomedical Engineering in Neuroscience* (pp. 197-220). Singapore: Springer Singapore.

Shoeb, A. (September 2009). Application of Machine Learning to Epileptic Seizure Onset Detection and Treatment. *PhD Thesis, Massachusetts Institute of Technology*,.

Shukla, A., & Majumdar, A. (2015). Exploiting inter-channel correlation in EEG signal reconstruction. *Biomedical Signal Processing and Control, 18*, 49-55. doi:https://doi.org/10.1016/j.bspc.2014.11.006

Silva, B. M. C., Rodrigues, J. J. P. C., de la Torre Díez, I., López-Coronado, M., & Saleem, K. (2015). Mobile-health: A review of current state in 2015. *Journal of Biomedical Informatics, 56*, 265-272. doi:https://doi.org/10.1016/j.jbi.2015.06.003

Tibshirani, R. (1996). Regression shrinkage and selection via the Lasso. *Journal of the Royal Statistical Society. Series B (Methodological), 58*(1), 267-288. Retrieved from www.jstor.org/stable/2346178

Tropp, J. A., & Gilbert, A. C. (2007). Signal recovery from random measurements via orthogonal matching pursuit. *IEEE Transactions on Information Theory, 53*(12), 4655-4666. doi:10.1109/TIT.2007.909108

Tropp, J. A., Gilbert, A. C., & Strauss, M. J. (2006). Algorithms for simultaneous sparse approximation. Part I: Greedy pursuit. *Signal Processing, 86*(3), 572-588. doi:https://doi.org/10.1016/j.sigpro.2005.05.030

World Health Organization. (2001). *Epilepsy. Fact sheet, World Health Organization, Geneva, Switzerland.* Retrieved from http://www.who.int/mediacentre/factsheets/fs999/en/

Zabihi M Fau - Kiranyaz, S., Kiranyaz S Fau - Jantti, V., Jantti V Fau - Lipping, T., Lipping T Fau - Gabbouj, M., & Gabbouj, M. (2020). Patient-specific seizure detection using nonlinear dynamics and Nullclines. *IEEE J Biomed Health Inform, 24 (2)*, 543-555.

Zeng, K., Yan, J., Wang, Y., Sik, A., Ouyang, G., & Li, X. (2016). Automatic detection of absence seizures with compressive sensing EEG. *Neurocomputing, 171*, 497-502. doi:https://doi.org/10.1016/j.neucom.2015.06.076

Zhang, Z., Jung, T., Makeig, S., & Rao, B. D. (2013). Compressed sensing of EEG for wireless telemonitoring with low energy consumption and inexpensive hardware. *IEEE Transactions on Biomedical Engineering, 60*(1), 221-224. doi:10.1109/TBME.2012.2217959

Zhang, Z., & Rao, B. D. (2013). Extension of SBL algorithms for the recovery of block sparse signals with intra-block correlation. *IEEE Transactions on Signal Processing, 61*(8), 2009-2015. doi:https://doi.org/10.1109/TSP.2013.2241055